Plant Cell Advance Publication. Published on November 14, 2018, doi:10.1105/tpc.18.00641

RESEARCH ARTICLE

Analysis of Two New Arabinosyltransferases Belonging to the Carbohydrate-Active Enzyme (CAZY) Glycosyl Transferase Family 1 Provides Insights into Disease Resistance and Sugar Donor Specificity

Thomas Louveau[a], Anastasia Orme[a], Hans Pfalzgraf[d], Michael J. Stephenson[a], Rachel Melton[a], Gerhard Saalbach[b], Andrew M. Hemmings[d], Aymeric Leveau[a], Martin Rejzek[b], Robert J. Vickerstaff[c*], Tim Langdon[c], Robert A. Field[b] and Anne Osbourn[a,1]

[a]Department of Metabolic Biology and [b]Department of Biological Chemistry, John Innes Centre, Norwich Research Park, Norwich NR4 7UH, UK; [c]Institute of Biological, Environmental and Rural Sciences, Aberystwyth University, Aberystwyth SY23 3FL, UK; [d]School of Biological Sciences, University of East Anglia, Norwich Research Park, Norwich NR4 7TJ, UK.
*Current address: East Malling Research, New Road, East Malling ME19 9BJ, UK.
[1]To whom correspondence may be addressed. Email: anne.osbourn@jic.ac.uk

Short title: Oat and soybean GT1 arabinosyltransferases

One sentence summary: Analysis of plant natural product arabinosyltransferases identifies determinants of sugar donor specificity and suggests convergent evolution in monocots and eudicots.

The author(s) responsible for distribution of materials integral to the findings presented in this article in accordance with the policy described in the Instructions for Authors (www.plantcell.org) is: Anne Osbourn (anne.osbourn@jic.ac.uk).

ABSTRACT

Glycosylation of small molecules is critical for numerous biological processes in plants, including hormone homeostasis, neutralization of xenobiotics, and synthesis and storage of specialized metabolites. Glycosylation of plant natural products is usually carried out by uridine diphosphate-dependent glycosyltransferases (UGTs). Triterpene glycosides (saponins) are a large family of plant natural products that determine important agronomic traits such as disease resistance and flavor and have numerous pharmaceutical applications. Most characterized plant natural product UGTs are glucosyltransferases, and little is known about enzymes that add other sugars. Here we report the discovery and characterization of AsAAT1 (UGT99D1), which is required for biosynthesis of the antifungal saponin avenacin A-1 in oat (*Avena strigosa*). This enzyme adds L-arabinose to the triterpene scaffold at the C-3 position, a modification critical for disease resistance. The only previously reported plant natural product arabinosyltransferase is a flavonoid arabinosyltransferase from *Arabidopsis thaliana*. We show that AsAAT1 has high specificity for UDP-β-L-arabinopyranose, identify two amino acids required for sugar donor specificity, and through targeted mutagenesis convert AsAAT1 into a glucosyltransferase. We further identify a second arabinosyltransferase potentially implicated in the biosynthesis of saponins that determine bitterness in soybean (*Glycine max*). Our investigations suggest independent evolution of UDP-arabinose sugar donor specificity in arabinosyltransferases in monocots and eudicots.

INTRODUCTION

Plants produce a huge array of natural products, many of which are glycosylated (Vetter, 2000; Vincken et al., 2007; Liu et al., 2013). Glycosylation can play a major role in the structural diversification of secondary metabolites. For example, over 300 glycosides have been reported for the simple flavonol quercetin alone (Reuben et al., 2006). Glycosylation modifies the reactivity and solubility of the corresponding aglycones, so influencing cellular localization and bioactivity (Augustin et al., 2011; Liu et al., 2013).

Plant natural products are decorated with a variety of different types of individual sugars and oligosaccharide chains. Studies involving various glycoconjugates of the same scaffold suggest that the identity of the sugar unit can have a major influence on bioactivity. For example, tests of six different monoglycosides of the sesquiterpene α-bisabolol against various cancerous cell lines for cytotoxicity revealed considerable variation in activity, with α-bisabolol rhamnoside being the most active (Piochon et al., 2009). Similarly, Bernard et al. (1997) showed that quercetin 3-*O*-α-L-rhamnopyranosyl-[1,6]-β-D-galactopyranoside was five time less effective in stimulating topoisomerase IV-dependent DNA cleavage than quercetin 3-*O*-α-L-rhamnopyranosyl-[1,6]-β-D-glucopyranoside, the two flavones differing only in the nature of the sugar unit attached to the C-3 position.

Glycosylation of plant natural products is usually carried out by uridine diphosphate-dependent glycosyltransferases (UGTs) belonging to the carbohydrate-active enzyme (CAZY) glycosyltransferase 1 (GT1) family (Vogt and Jones, 2000; Bowles et al., 2006). These enzymes transfer sugars from uridine diphosphate-activated sugar moieties to small hydrophobic acceptor molecules. Over the last 15 years, considerable effort has been invested in the functional characterization of multiple UGTs from a variety of plant species. UGTs generally show high specificity for their sugar donors and recognize a single uridine diphosphate (UDP)-activated sugar as their substrate (Kubo et al., 2004; Bowles et al., 2006; Osmani et al., 2008; Noguchi et al., 2009). Plant UGTs recognize their sugar donors via a motif localized on the C-terminal part of the enzyme. This Plant Secondary Product Glycosyltransferase (PSPG) motif is highly conserved throughout UGT families (Hughes and Hughes, 1994; Mackenzie et al., 1997; Ross et al., 2001). Most characterized plant UGTs use

UDP-α-D-glucose (UDP-Glc) as their sugar donor, although several UGTs that use alternative sugars have also been reported (Bowles et al., 2006; Osmani et al., 2009).

Triterpene glycosides (also known as saponins) are one of the largest and most structurally diverse groups of plant natural products. These compounds are synthesized from the isoprenoid precursor 2,3-oxidosqualene and share a common biogenic origin with sterols. They protect plants against pests and pathogens and can determine other agronomically important traits such as flavor. They also have a wide range of potential medicinal and industrial applications (Augustin et al., 2011; Sawai and Saito, 2011). Saponins commonly have a sugar chain attached at the C-3 position that may consist of up to five sugar molecules, and sometimes additional sugar chains located elsewhere on the molecule. These sugars are varied and diverse, including D-glucose, D-galactose, L-arabinose, D-glucuronic acid, D-xylose, L-rhamnose, D-fucose, and D-apiose. Glycosylation is critical for many of the bioactive properties of these compounds (Osbourn, 1996; Francis et al., 2002).

Despite the importance of glycosylation for biological activity, characterization of triterpenoid UGTs has so far been limited. Of the 19 triterpenoid UGTs reported so far, 15 are D-glucosyltransferases. A further three hexose transferases have also been identified, transferring D-glucuronic acid, D-galactose and L-rhamnose, respectively, and only one pentose (D-xylose) transferase (Supplemental Table 1). The discovery of enzymes that are able to add other diverse sugars and investigation of the features that determine preference for different sugar donors will enable a wider array of triterpenoid glycoforms to be engineered. These advances, along with improved understanding of the significance of sugar chain composition for bioactivity, will open up new opportunities to fully exploit glycodiversification for agronomic, medicinal and industrial biotechnology applications.

Previously we carried out a forward screen for sodium azide-generated mutants of diploid oat (*Avena strigosa*) that are unable to synthesize triterpene glycosides known as avenacins (Figure 1A) (Papadopoulou et al., 1999). Avenacins are antimicrobial compounds that are produced in oat roots and that provide protection against soil-borne fungal pathogens, including the causal agent of take-all disease of cereals, *Gaeumannomyces graminis* var. *tritici* (Papadopoulou et al., 1999), a disease responsible for major yield losses in all wheat-growing areas of the world.

The major avenacin found in oat roots is avenacin A-1. Previously we have characterized five of the genes in the avenacin pathway, which form part of a biosynthetic gene cluster (Haralampidis et al., 2001; Owatworakit et al., 2012; Geisler et al., 2013; Mugford et al., 2013). These include genes encoding enzymes for the biosynthesis and oxidation of the triterpene scaffold β-amyrin (*AsbAS1/Sad1* and *AsCYP51H10/Sad2*, respectively) (Haralampidis et al., 2001; Geisler et al., 2013), and for synthesis and addition of the UV-fluorescent *N* -methyl anthranilate acyl group at the C-21 position (*AsMT1/Sad9*, *AsUGT74H5/Sad10* and *AsSCPL1/Sad7*) (Owatworakit et al., 2012; Mugford et al., 2013) (Figure 1C). Avenacin A-1 has a branched sugar chain at the C-3 position. This sugar chain is essential for antimicrobial activity, rendering the molecule amphipathic and so enabling it to disrupt fungal membranes (Osbourn et al., 1995; Armah et al., 1999). The first sugar in the sugar chain is L-arabinose, which is linked to two D-glucose molecules via 1-2 and 1-4 linkages. The enzymes required for avenacin glycosylation have not yet been characterized. No triterpene arabinosyltransferase has as yet been identified, and the only plant natural product arabinosyltransferase known is a flavonoid arabinosyltransferase (UGT78D3) from *Arabidopsis thaliana* (Yonekura-Sakakibara et al., 2008).

Here we report the discovery of AsAAT1 (UGT99D1), the enzyme that catalyses the addition of the first sugar in the avenacin oligosaccharide chain. AsAAT1 is the first triterpene arabinosyltransferase to be characterized, and only the second reported plant GT1 arabinosyltransferase. We demonstrate that AsAAT1 shows high specificity for UDP-β-L-arabinopyranose (UDP-Ara) as its sugar donor and identify two amino acid residues mutually required for sugar donor specificity. We subsequently use this knowledge to identify a second triterpenoid arabinosyltransferase (GmSSAT1) implicated in the synthesis of triterpene glycosides that determine bitterness and anti-feedant activity in soybean (*Glycine max*). Although the oat AsAAT1, soybean GmSSAT1 and AtUGT78D3 enzymes are phylogenetically distinct, they all harbor the same signature histidine residue critical for arabinosylation activity, suggesting independent evolution of sugar donor specificity in plant natural product arabinosyltransferases in monocots and eudicots.

RESULTS

Identification of candidate UGTs expressed in oat root tips

Avenacin A-1 is synthesised in the epidermal cells of oat root tips (Haralampidis et al., 2001; Mugford et al., 2009). To identify candidate UGTs implicated in avenacin biosynthesis, we mined an oat root tip transcriptome database that we generated previously (Kemen et al., 2014) using BLAST analysis (tBLASTn). The mRNA used to generate this transcriptome resource was extracted from the terminal 0.5 cm of the root tips of young oat seedlings, i.e. from avenacin-producing tissues. Representative sequences for each of the 21 subfamilies of plant UGTs present in *A. thaliana* were used as query sequences (Supplemental Table 2). The resulting hits were then assessed manually using alignment tools to eliminate redundant sequences. A total of ~100 unique UGT-like sequences were identified, 36 of which were predicted to correspond to entire coding sequences (Supplemental Table 3).

Phylogenetic analysis of the full-length UGT coding sequences was then carried out (Figure 2A). Four sequences corresponding to the highly conserved sterol glycosyltransferase (UGT80) and monogalactosyldiacylglycerol synthase (UGT81) groups (Grille et al., 2010; Caputi et al., 2011) (Supplemental Table 3) were omitted to avoid skewing the phylogeny reconstruction. The predicted amino acid sequences of the oat UGTs were aligned with those of characterized UGTs from other plants, including those previously reported to glycosylate triterpenoids (Supplemental Table 4 and Supplemental Data set 1). The tree approximately recapitulated the monophyletic groups A-O previously defined by Li et al. (2001), but inclusion of the oat UGTs broadened the architecture to reveal oat-specific subfamilies. The oat UGTs (shown in red) were distributed across the phylogeny but were particularly well represented in groups D, E, and L. Of these, we have previously characterized three group L oat UGTs (AsUGT74H5/SAD10, AsUGT74H6, and AsUGT74H7) and shown that AsUGT74H5/SAD10 and AsUGT74H6 are required for the generation of the acyl glucose donors (*N*- methyl anthranilate β-D-glucose and benzoic acid β-D-glucose, respectively) used by the serine carboxypeptidase-like acyltransferase AsSCPL1/SAD7 for biosynthesis of avenacins (Owatworakit et al., 2012; Mugford et al., 2013).

In parallel with our transcriptome-mining approach we also carried out proteomic analysis of the tips and elongation zones of oat roots (Supplemental Figure 1). The previously characterized avenacin biosynthetic enzyme AsUGT74H5 (SAD10)

(Owatworakit et al., 2012) showed higher accumulation in the root tips relative to the elongation zone. Of the 26 other UGT proteins detected in oat roots, three also accumulated at higher levels in the root tips compared with the elongation zone (AsUGT93B16, AsUGT99D1 and AsUGT706F7).

Eleven of the 19 triterpene UGTs that have previously been characterized from various plant species belong to UGT group D (Supplemental Table 1) (Achnine et al., 2005; Meesapyodsuk et al., 2007; Naoumkina et al., 2010; Shibuya et al., 2010; Augustin et al., 2012; Sayama et al., 2012; Dai et al., 2015; Wang et al., 2015; Wei et al., 2015; Xu et al., 2016). We prioritized the six oat GTs from group D for gene expression analysis, along with the phylogenetically related enzyme AsUGT705A4, as well as AsUGT93B16 (group O) and AsUGT706F7 (group E), selected based on proteomic analysis. Six of these nine candidate genes had similar expression patterns to the characterized avenacin biosynthetic genes (*AsUGT74H5/Sad10* is included as an example) (Figure 2B). All nine candidate UGTs were taken forward for functional analysis (Table 1).

Heterologous expression and *in vitro* activities of candidate UGTs

The coding sequences for the nine candidate genes were amplified from oat root tip complementary DNA (cDNA) and cloned into the expression vector pH9GW via the Gateway system (Hartley et al., 2000). The first sugar in the avenacin oligosaccharide chain is L-arabinose (Figure 1). To investigate whether any of the candidate enzymes showed a preference for UDP-Ara as a sugar donor, the UGTs were expressed as recombinant N-terminal 9xhistidine-tagged proteins in *Escherichia coli*. Following lysis, protein preparations enriched for the recombinant enzymes were prepared using Immobilized Metal Affinity Chromatography (IMAC) (Supplemental Figure 2A). The resulting preparations were incubated with each of three different sugar donors [UDP-Glc, UDP-α-D-galactose (UDP-Gal) or UDP-Ara] and 2,4,5-trichlorophenol (TCP). TCP was chosen as a universal acceptor in these assays because previous studies have shown that many UGTs are able to glycosylate TCP as well as their natural acceptor (Messner et al., 2003). The previously characterized *A. thaliana* flavonoid arabinosyltransferase UGT78D3 (Yonekura-Sakakibara et al., 2008) and oat *N*-methyl anthranilate glucosyltransferase AsUGT74H5 (SAD10) (Owatworakit et al., 2012) were included

as controls. These two enzymes produced TCP arabinoside and TCP glucoside, respectively, as expected (Figure 3A). Of the nine candidate UGTs, only AsUGT99D1 showed a preference for UDP-Ara. This enzyme did not give any detectable product when UDP-Gal or UDP-Glc were supplied as potential sugar donors. The other UGTs showed a preference for UDP-Glc and so are likely to be glucosyltransferases (with the exception of AsUGT705A4, for which no activity was observed) (Figure 3A).

Incubation of the AsUGT99D1 enzyme preparation with the avenacin pathway intermediate 12,13β-epoxy-16β-hydroxy-β-amyrin (EpHβA) led to a new product when UDP-Ara was supplied as the sugar donor (Supplemental Figure 2B). Products were not detected with β-amyrin, suggesting that oxygenation of this scaffold is needed for AsUGT99D1 to act. When UDP-Glc was supplied as a potential sugar donor only a very small amount of conversion of EpHβA was observed, while no product was detected with UDP-Gal (Supplemental Figure 2B).

To further investigate the function of AsUGT99D1, we carried out acid hydrolysis of purified avenacin A-1 to remove the C-3 trisaccharide. Liquid chromatography-mass spectrometry (LC-MS) analysis confirmed that the blue fluorescent hydrolysis product generated had a mass corresponding to deglycosylated avenacin (*m/z* $[M+H]^+$ 638.1), with complete consumption of avenacin A-1 (*m/z* $[M+H]^+$ 1094.1) (Figure 3B**,** left and middle panels). After incubation of this hydrolysis product with recombinant AsUGT99D1 and UDP-Ara, a new fluorescent product was detected that had a mass consistent with addition of a pentose (*m/z* $[M+H]^+$ 770.1) (Figure 3B**,** right panel). These results suggest that AsUGT99D1 is able to initiate assembly of the sugar chain of avenacin A-1 by addition of L-arabinose.

Transient expression of AsUGT99D1 in *Nicotiana benthamiana*

Previously we have shown that *Agrobacterium*-mediated transient expression of triterpene synthase and cytochrome P450 biosynthetic genes in *Nicotiana benthamiana* leaves enables rapid production of milligram to gram-scale amounts of simple and oxygenated triterpenes (Geisler et al., 2013; Mugford et al., 2013; Reed et al., 2017). We therefore used this expression system to carry out functional analysis of the candidate avenacin arabinosyltransferase enzyme AsUGT99D1 *in planta*. The AsUGT99D1 coding sequence was introduced into a Gateway-

compatible pEAQ-Dest1 vector for co-expression with earlier enzymes in the avenacin pathway.

In accordance with previous work, co-expression of the first and second steps in the avenacin pathway (AsbAS1/SAD1 and AsCYP51H10/SAD2, respectively; hereafter referred to as SAD1 and SAD2) yielded accumulation of the early avenacin pathway intermediate EpHβA, which was readily detectable by GC-MS (Figure 4A). In contrast, when SAD1 and SAD2 were co-expressed with AsUGT99D1, the levels of EpHβA were markedly reduced (Figure 4A) and a new more polar product was detected by HPLC coupled to charged aerosol detector (CAD) (Figure 4B). This new product was not present in extracts from leaves that had been infiltrated with the SAD1 and AsUGT99D1 expression constructs in the absence of SAD2 (Figure 4B). Furthermore, it had the same retention time (t_R 12.0 min) as the product generated *in vitro* following incubation of EpHβA together with recombinant AsUGT99D1 (Supplemental Figure 3).

To identify the product generated by co-expression of SAD1, SAD2 and AsUGT99D1 in *N. benthamiana*, we scaled up our transient expression experiments. Vacuum infiltration of 44 *N. benthamiana* plants was carried out, and the freeze-dried leaf material extracted by pressurized solvent extraction. The triterpenoid product was purified using flash chromatography in normal and reverse phase mode. A total of 5.45 mg of product was obtained and estimated to be 94.5% pure using a CAD detector (corresponding to a yield of 0.79 mg/g dry weight) (Supplemental Figure 3). The structure of this product was analyzed by nuclear magnetic resonance (NMR) spectroscopy, and the ^{1}H and ^{13}C NMR spectra fully assigned using a combination of COSY, DEPT-edited HSQC, and HMBC experiments (Supplemental Figure 4). The data are consistent with the structure being 16β-hydroxy-β-amyrin 3-*O*-α-L-arabinoside (Figure 4C). Importantly, an HMBC correlation was observed between the C-1' hydrogen of the sugar moiety and the C-3 methine type carbon of the triterpene scaffold, confirming the site of glycosylation (Figure 4C, Supplemental Figure 4). Collectively our data suggest that AsUGT99D1 is the missing avenacin arabinosyltransferase (hereafter named AsAAT1).

AsAAT1 mutants of oat are compromised in avenacin biosynthesis and have enhanced susceptibility to take-all disease

Our collection of avenacin-deficient mutants of *A. strigosa* consists of ~100 mutants, around half of which have been assigned to characterized loci (Papadopoulou et al., 1999; Qi et al., 2004; Qi et al., 2006; Mylona et al., 2008; Mugford et al., 2009; Qin et al., 2010; Owatworakit et al., 2012; Geisler et al., 2013; Mugford et al., 2013). We sequenced the *AsAAT1* gene in 47 uncharacterized avenacin-deficient mutants and identified a single line (#807) with a mutation in the *AsAAT1* coding sequence. This mutation is predicted to give rise to a premature stop codon (Supplemental Figure 5A). Thin layer chromatography (TLC) analysis revealed that the levels of avenacin A-1 were substantially reduced in root extracts of this mutant (Supplemental Figure 5B). Subsequent analysis of seedlings of 139 F_2 progeny derived from a cross between the wild-type *A. strigosa* parent and the mutant #807 line confirmed that the reduced avenacin phenotype co-segregated with the single nucleotide polymorphism in the *AsAAT1* gene, and that the avenacin-deficient phenotype of mutant #807 is likely to be due to a recessive mutant allele of *AsAAT1* (Supplemental Figure 5C; Table 2).

The previously characterized avenacin biosynthetic genes are physically clustered in the *A. strigosa* genome (Mugford et al., 2013). An accession of another avenacin-producing diploid oat species, *Avena atlantica* (IBERS Cc7277), has been the target of whole genome shotgun sequencing, with subsequent mapping of assembled contigs by survey resequencing of recombinant inbred progeny derived from a cross between this accession and *A. strigosa* accession Cc7651 (IBERS) (Vickerstaff and Langdon, unpublished). A single orthologue of *AsAAT1* contained on a contig of 14,086 bp was identified in the *A. atlantica* assembly (Supplemental Data set 2). This contig is closely linked to the *Sad2* locus, while the other 8 UGT genes selected earlier are not (Supplemental Table 5). This suggests that *AsAAT1* is likely to be part of the extended avenacin cluster. Future work will shed light on the full extent of the avenacin biosynthetic gene cluster and on the degree of conservation across different oat species.

Avenacins A-1, B-1, A-2 and B-2 (Figure 1A) were readily detectable by HPLC analysis in extracts of wild-type oat roots (Figure 5A). In contrast, the levels of all four were markedly reduced in the *aat1* mutant line #807, and two new smaller peaks of more polar compounds were observed (Figure 5A). Formate and chloride adducts (*m/z* 524.8 and 535.0 respectively) (Supplemental Figure 5D, left panel) of

the most apolar of these (t_R 11.4 min) correspond to a compound with a molecular weight of 490 Da. The apparent mass and polarity of this compound, as well as its lack of UV fluorescence, implies that *aat1* accumulates the avenacin aglycone lacking the acyl group and the C-30 aldehyde. The other new peak (t_R 6.3 min) has a molecular weight that corresponds to the first product plus two hexoses (814.5 Da) (Supplemental Figure 5D, right panel). A minor peak corresponding to the monoglucoside could also be detected at 7.7 min (652.4 Da) (Supplemental Figure 5D, central panel). These more polar products may be a result of further modification of the avenacin intermediate by non-specific glycosyltransferases in the absence of the functional AsAAT1 arabinosyltransferase. Low levels of avenacins were still detected, suggesting that other background enzymes may also be able to partially substitute for AsAAT1 in *aat1* mutant lines.

F_2 lines homozygous for the *aat1* mutation did not have any obvious root phenotype other than reduced fluorescence, indicating that mutation of *AsAAT1* is unlikely to affect root growth and development (Supplemental Figure 5C). Since glycosylation is known to be critical for the antifungal activity of avenacins, we investigated the effects of mutation at *AsAAT1* on disease resistance. Disease tests revealed that the *aat1* mutant had enhanced susceptibility to take-all disease, consistent with a role for AsAAT1 in disease resistance (Figure 5B; Supplemental Figure 5E).

Prediction and validation of a soybean arabinosyltransferase based on specific features of AsAAT1

The most closely related UGT to AsAAT1 in oat is AsUGT99A6 (Figure 2A), which is a glucosyltransferase, based on our TCP assays (Figure 3A). In *A. thaliana* the closest relative of AtUGT78D3 (AtUGT78D2) is also a glucosyltransferase (Tohge et al., 2005). Oat AsAAT1 and *A. thaliana* AtUGT78D3 both have a histidine (H) residue at the C-terminal end of the PSPG motif, while their glucosyltransferase counterparts have glutamine (Q) in this position (Figure 6A). This glutamine residue has been shown to be involved in sugar donor selectivity and is highly conserved in many plant UGTs (Kubo et al., 2004; Gachon et al., 2005; Caputi et al., 2008). Replacement of the histidine residue in AtUGT78D3 with glutamine has previously been shown to result in gain of ability to recognize UDP-xylose and UDP-glucose and loss of ability to recognize UDP-arabinose (Han et al., 2014). We therefore

reasoned that the presence of a histidine residue in this position may be indicative of arabinosyltransferase activity.

Soybean produces triterpene glycosides known as soyasaponins. Group A soyasaponins have a branched sugar chain attached at the C-22 position initiated by an L-arabinose residue (Figure 1B). The enzyme responsible for the addition of this L-arabinose is not known. We mined the soybean genome (http://www.soybase.org/) for candidate arabinosyltransferase genes by searching with a modified PSPG consensus motif containing a histidine residue at the critical position using tBlastn. Six sequences were identified (Supplemental Table 6). Two of these belong to group D (Figure 6B). One of these - GmUGT73P2 (GmSGT2) - has previously been characterized as a soyasapogenol B 3-*O*-glucuronide galactosyltransferase (Shibuya et al., 2010). The other shares ~53% amino acid sequence identity with the *Medicago truncatula* soyasaponin glucosyltransferase UGT73K1 (Supplemental Table 6) (Achnine et al., 2005).

The coding sequence of this latter gene was synthesized commercially and cloned into the pH9-GW vector for expression in *E. coli*. Soluble recombinant *N*-term-9xHis-tagged enzyme was produced and enriched using Ni-NTA resin. The recombinant enzyme was incubated with soyasaponin I as an acceptor, together with each of three potential sugar donors, UDP-Glc, UDP-Gal and UDP-Ara, and reaction products were analysed by LC-CAD/MS. Only one major product was detected by CAD in the presence of UDP-Ara. This product was absent when UDP-Gal or UDP-Glc were supplied as sugar donors (Figure 7A). The mass of the new product (*m/z* 1073.5 by HR-MS) is consistent with arabinosylation (132.1 Da) of soyasaponin I (941.2 Da) (Supplemental Figure 6A). We therefore named this enzyme GmSSAT1 (*G. max* SoyaSaponin ArabinosylTransferase 1; GmSSAT1).

A UGT (GmUGT73F2) that extends the sugar chain at the C-22 position of soyasaponin by adding D-glucose to the L-arabinose group has previously been discovered (Sayama et al., 2012). When recombinant GmUGT73F2 was incubated with UDP-Glc and the product of GmSSAT1, a new product was detected with a molecular mass corresponding to the glucoside of the former product (Figure 7B, Supplemental Figure 6B). GmUGT73F2 was inactive when incubated with UDP-Glc and soyasaponin I. Together, those results suggest that GmSSAT1 and GmUGT73F2 act consecutively in the initiation and extension of the sugar chain at

the C-22 carbon position of group A soyasaponins (Figure 7C). *GmSSAT1* is co-expressed with *GmUGT73F2*, most notably in the pods and pod shells where soyasaponins accumulate, suggesting a role for GmSSAT1 in the biosynthesis of these bitter compounds (Supplemental Figure 6C).

Site directed mutagenesis of *AsAAT1*

In addition to the histidine residue at the C-terminal end of the PSPG motif, a single amino acid difference was also observed between AsAAT1 (proline) and AsUGT99A6 (serine) in the middle of the N-terminus loop positioned between the fifth β-strand and the fifth α-helix [the N5 loop, as defined by Osmani et al. (2009)] (Figure 6A). The N5 loop has been shown to be involved in sugar specificity of the triterpene glucosyltransferase MtUGT71G1 from *M. truncatula*, soyasaponin glucosyltransferase GmUGT73F2 (mentioned earlier) and a flavonoid glucuronosyltransferase from *Perilla frutescens* (UGT88D7) (Kubo et al., 2004; He et al., 2006; Noguchi et al., 2009). To further investigate the basis of AsAAT1 sugar donor preference, a homology model was generated using the online software I-TASSER (Yang et al., 2015) and MODELLER (Sali and Blundell, 1993) was used to refine the N-terminal loop of AsAAT1 PSPG motif. Docking of UDP-Ara into the sugar donor binding site of AsAAT1 was consistent with the arabinoside moiety of UDP-Ara having a hydrogen bond to His404 (bond length 2.8 Å) and a hydrophobic interaction with Pro154 (Figure 8A).

We carried out site directed mutagenesis of AsAAT1 to convert His404 and Pro154 to the corresponding residues found in the glucosyltransferase AsUGT99A6 (glutamine and serine, respectively). Purified N-terminal 9xHis-tagged recombinant wild-type AsAAT1, the mutant forms H404Q and P154S, and the double mutant H404Q-P154S were assayed for their ability to glycosylate the avenacin aglycone (Supplemental Figure 7A). The AsAAT1-H404Q mutant had reduced arabinosyltransferase activity compared to the wild-type enzyme, and increased xylosyl- and glucosyltransferase activities, i.e. showed greater promiscuity for different sugar donors (Figure 8B). When Pro154 was mutated to serine, arabinosylation was still the predominant activity, but galactosyl transferase activity increased (Figure 8B). UDP-Gal was therefore a better donor for the P154S mutant variant than UDP-xylose or UDP-glucose. The double mutant AsAAT1-H404Q-

P154S preferred UDP-Glc over the three other sugar donors (Figure 8B); glucosyltransferase activity was ~10-fold higher than that of wild-type AsAAT1, while arabinosyltransferase activity decreased markedly (~30 fold).

The effects of the H404Q, P154S and H404Q-P154S mutations on AsAAT1 sugar specificity were also examined in *N. benthamiana* by expressing wild-type AsAAT1 or the mutant variants with SAD1 and SAD2 and analyzing leaf extracts by HPLC-CAD (Figure 8C). These analyses were supported by LC-MS analysis of leaf extracts and *in vitro* reactions in which the wild-type and mutant AsAAT1 enzymes were incubated with different sugar nucleotide donors (Supplemental Figure 7C). HPLC-CAD analysis of extracts from leaves expressing wild-type AsAAT1 revealed the accumulation of EpHβA-Ara, as expected (Figure 8C). In contrast, the H404Q-P154S double mutant yielded EpHβA-Glc, confirming conversion of AsAAT1 to a glucosyltransferase (Figure 8C); no other EpHβA glycosides could be detected (Supplemental Figure 7C). Expression of the H404Q mutant yielded EpHβA-Ara, EpHβA-Glc, and traces of EpHβA-Xyl (Figure 8C; Supplemental Figure 7C), while P154S produced primarily EpHβA-Ara with traces of EpHβA-Gal and -Glc (Figure 8C; Supplemental Figure 7C).

DISCUSSION

AsAAT1 is part of the avenacin pathway

Glycosylation has profound effects on the biological activities of natural products. UGTs belonging to the CAZY GT1 family are critical for small molecule glycosylation in plants. The trisaccharide moiety attached to the avenacin scaffold is essential for antifungal activity and hence disease resistance. Here we mine an oat root transcriptome database for candidate UGTs implicated in avenacin biosynthesis and report the discovery and characterization of the GT family 1 triterpenoid arabinosyltransferase AsAAT1. This enzyme initiates the addition of the avenacin oligosaccharide chain through addition of L-arabinopyranose at the C-3 position of the triterpene scaffold. Glycosylation of the avenacin scaffold is critical for antifungal activity (Mylona et al., 2008). Consistent with this, *aat1* mutants of *A. strigosa* have enhanced susceptibility to *G. graminis* var. *tritici*, the causal agent of the take-all disease. Biochemical analysis suggests that the avenacin pathway intermediate that

accumulates in the roots of *aat1* mutants is deglycosyl-, desacyl-avenacin minus the C-30 aldehyde. This intermediate seems to be subject to further modification in the mutant background, including two successive glycosylation events. The apparent lack of the C-30 aldehyde in the intermediate coupled with *in vitro* assays with early intermediates of the pathway, suggest that AsAAT1 requires β-amyrin oxidation and that arabinosylation is a prerequisite for C-30 oxidation. This places AsAAT1 somewhere between SAD2 and a hypothetical arabinoside glucosyltransferase or C-30 oxidase (Figure 1C). Most likely, arabinosylation catalysed by AsAAT1 occurs in the cytosol after oxidation of the oleanane scaffold. C-30 oxidation and addition of the two D-glucose molecules to the C-3 L-arabinose are then necessary prior to acylation in the vacuole by the serine carboxypeptidase-like (SCPL) acyl transferase SAD7 (Mugford et al., 2009).

Avenacins are still detectable in root extracts of the *aat1* mutant albeit at considerably reduced levels, suggesting that another oat enzyme may be partially redundant with AsAAT1. Functional redundancy coupled with non-specific glucosylation of the *aat1* intermediate (Figure 5A) may alleviate accumulation of toxic intermediates, preventing the severe root development phenotypes seen in other avenacin mutants affected in glucosylation (Mylona et al., 2008).

GmSSAT1, an arabinosyltransferase implicated in the biosynthesis of soyasaponins that determine bitterness in soybean

In vitro assays performed with recombinant soybean UGTs suggest that GmSSAT1 and UGT73F2 are likely to act consecutively in initiation and extension of the sugar chain at the C-22 carbon position of group A saponins from soybean (Ab, Ac, Ad, Af and Ah; Figure 7C). Both genes are co-expressed in soybean pods (Supplemental Figure 6C). The predicted natural acceptor of GmSSAT1 (non-acetylated non-arabinosylated soyasaponin A0-αg) is not commercially available, and the full function of this enzyme in soyasaponin biosynthesis remains to be elucidated. However, *GmSSAT1* represents a potential target for plant breeding in endeavours to generate non-bitter soybean varieties. The arabinosyltransferase involved in soyasaponin biosynthesis adds the first sugar of the C-22 sugar chain present in group A saponins. The acetylated sugars attached via L-arabinose at this position

are thought to be responsible for the bitterness and astringent aftertaste of soybean (Sayama et al., 2012).

New insights into determinants of sugar donor selectivity

The only other GT1 family arabinosyltransferase to have been characterized from plants prior to our work is the flavonoid arabinosyltransferase UGT78D3 from *A. thaliana*. AsAAT1, GmSSAT1 and UGT78D3 all have a conserved histidine residue at the end of the PSPG signature motif, while their most closely related glycosyltransferase counterparts do not (Figure 6A). It is interesting to note that AsAAT1 and GmSSAT1 belong to different clades of group D (Figure 6B), while *A. thaliana* UGT78D3 is in group F (Figure 2A), suggesting independent evolution of sugar donor specificity in GT1 arabinosyltransferases in monocots and eudicots. Through comparative analysis, protein modelling and mutagenesis we have shown that this histidine residue (H404) is critical for sugar donor specificity in AsAAT1, and that mutation of H404 and P154 is sufficient to convert AsAAT1 from an arabinosyltransferase to a glucosyltransferase.

Molecular modelling suggests that P154 is in close proximity with the CH_2 of the C-5 position of UDP-Ara (5.2 Å distance, Figure 8A). A potential steric constraint/hydrophobic interaction provided by the proline may thus favor accommodation of pentoses while preventing accommodation of hexoses. Replacement of P154 by serine could allow formation of a hydrogen bond with the C-6 hydroxyl group of hexoses, consistent with predictions from the crystal structure of the rice UGT Os79, where a serine in the equivalent position forms a H-bond with C-6 of glucose (Wetterhorn et al., 2016). Direct interaction of H404 with the C-4 hydroxy group of L-arabinose is not suggested by the 3D model (Figure 8A). Nevertheless, the modified activity of the H404Q mutant is consistent with previous reports on plant glycosyltransferases (Kubo et al., 2004; Han et al., 2014) and suggests that H404 may modify the orientation of the hemiacetal ring, so indirectly impacting on selectivity for C-4 stereochemistry (see Supplemental Figure 7B for sugar stereochemistry).

AsAAT1 is also unusual in having a two-amino acid insertion (I400 and G401) towards the C-terminal part of the PSPG motif (Figure 6A). To our knowledge this is a unique feature of AsAAT1. All plant UGTs characterized to date have a PSPG

motif 44 amino acids long (see Supplemental Data set 1 for large-scale alignment). However, we were unable to detect activity following either deletion of these two amino acids or replacement with the PSPG motif of AsUGT99A6. The 3D model of AsAAT1 suggests that those two residues may shape the region of the sugar donor binding pocket (Figure 8A). Those two residues could therefore also be involved in determining the sugar specificity of AsAAT1. The conformation of the loop from W396 to S402 was refined in MODELLER (Sali and Blundell, 1993) to accommodate the presence of these two additional amino acids, and the six best-scoring conformations subjected to energy minimization in order to optimize the AsAAT1 model.

The gain of knowledge in molecular mechanisms underlying sugar specificity in UGTs provided by this work along with previous work on other GT1 enzymes opens up opportunities to identify candidate glycosyltransferases with particular sugar donor preferences based on sequence information, as we have demonstrated here through identification of the new arabinosyltransferase GmSSAT1. Similar approaches may prove useful to identify the swathe of as-yet uncharacterized enzymes involved in the assembly of complex sugar chains of saponins and other glycosides.

Harnessing sugar specificity is crucial for glycodiversification

Glycosylation has profound effects on the biological activities, physical properties and compartmentalization of natural products. The discovery of family 1 GTs that add different types of sugars to plant natural products will be key for understanding and harnessing natural product glycosylation. Here we report two arabinosyltransferases from the GT1 family: AsAAT1, a C-3 triterpenoid arabinosyltransferase from oat and GmSSAT1, a C-22 triterpenoid arabinosyltransferase from soybean. Key residues for sugar donor specificity were identified via site-directed mutagenesis, allowing complete conversion of AsAAT1 from arabinosyltransferase to glucosyltransferase activity. This increased knowledge of the structural bases underlying sugar donor preference in family 1 GT enzymes can now be exploited to create new biocatalysts and enable unprecedented glycodiversification of natural products.

Of note, unlike yeast, the *N. benthamiana* transient expression platform is able to furnish an endogenous supply of UDP-Ara as well as UDP-Gal or UDP-Xyl, and so offers considerable potential as a system for glycodiversification of plant metabolites and small pharmaceuticals. Transient plant expression is demonstrably scalable and is currently used for production of pharmaceutical proteins by various companies (Sack et al. 2015). We have already used *N. benthamiana* transient expression to rapidly generate gram-scale quantities of triterpenoids in our lab (Reed et al., 2017). Given the potential for commercial scale up, this platform has the potential to be a disruptive technology for metabolic engineering of triterpenes and potentially also other high-value chemicals.

MATERIALS AND METHODS

Plant material. The wild-type *Avena strigosa* accession S75 and avenacin-deficient mutants were grown as described previously (Papadopoulou et al., 1999). Briefly, seeds of *A. strigosa* were surface sterilized with 5% sodium hypochlorite and then germinated at 22°C, 16 hours of light on damp filter paper after synchronization at 4°C for 24 hours in the dark. *Nicotiana benthamiana* plants were grown in green-houses maintained at 23- 25°C with 16 hours of supplementary light per day, as previously described (Sainsbury et al., 2012).

RNA and cDNA preparation. The cDNA used for amplification and subsequent cloning of the selected oat UGT genes and for gene expression analysis was generated from 3-day-old *A. strigosa* seedlings tissues. Total RNA was extracted using the RNeasy Plant Mini kit (Qiagen). First-strand cDNA synthesis was carried out from 1 µg of DNase-treated RNA using SuperScript II Reverse Transcriptase (Invitrogen).

Phylogenetic analysis. Representative amino acid sequences of characterized family 1 plant UGTs were collected from the Carbohydrate-Active enZymes (CAZy) database (http://www.cazy.org/). These sequences were augmented with sequences of characterized plant triterpenoid/steroidal UGTs. All sequences are listed in Supplemental Table 4. Deduced amino acid sequences derived from the predicted full-length *A. strigosa* UGT coding sequences (Supplemental Table 3) were incorporated into the phylogenetic reconstruction. Sequences were aligned using MUSCLE (http://www.ebi.ac.uk/Tools/msa/muscle/; Supplemental Data set 1). The unrooted phylogenetic tree was constructed using MEGA 5 (http://www.megasoftware.net/) by the neighbor-joining method with 1000 bootstrap replicates. Phylogenetic reconstruction of group D UGTs in Figure 5A was carried out using the same method.

Proteomic analysis. The tips and elongation zones of 5-day-old *A. strigosa* seedlings were harvested and approximately 30 mg of material was ground in liquid nitrogen using a pre-chilled mortar and pestle. Protein extraction was performed following previously published methods (Owatworakit et al., 2012) and concentrations determined using the Bradford method (Bradford, 1976) with bovine serum albumin (BSA, Sigma) as a standard. Samples (8 µg) were denatured at 95°C

for 15 min in the presence of Nupage reducing agent (Invitrogen) and separated using a precast polyacrylamide gel (Nupage 4-12% Bis-TRIS, Invitrogen) in 3-(*N*-morpholino) propanesulfonic acid (MOPS) buffer (Invitrogen).

To increase the relative abundance of UGT proteins and simplify the sample mixture we performed on-gel size-fractionation of proteins, taking advantage of the conserved length of UGTs (AsUGTs MW 48-55 kDa). Proteins with molecular weights of 45-57 kDa were excised from the SDS-PAGE gel with sterile razor blades. Gel slices were treated with DTT and iodoacetamide, and digested with trypsin according to standard procedures.

Peptides were extracted from the gels and analyzed by LC-MS/MS on an Orbitrap-Fusion™ mass spectrometer (Thermo Fisher, Hemel Hempstead, UK) equipped with an UltiMate™ 3000 RSLCnano System using an Acclaim PepMap C18 column (2 µm, 75 µm x 500 mm, Thermo). Aliquots of the tryptic digests were loaded and trapped using a pre-column which was then switched in-line to the analytical column for separation. Peptides were eluted with a gradient of 5-40% acetonitrile in water/0.1% formic acid at a rate of 0.5% min^{-1}. The column was connected to a 10 µm SilicaTip™ nanospray emitter (New Objective, Woburn, MA, USA) for infusion into the mass spectrometer. Data dependent analysis was performed using parallel top speed HCD/CID fragmentation method with the following parameters: 3 s cycle time, positive ion mode, orbitrap MS resolution = 60k, mass range (quadrupole) = 350-1550 m/z, MS2 isolation window 1.6 Da, charge states 2-5, threshold 3e4, AGC target 1e4, max. injection time 150 ms, dynamic exclusion 2 counts within 10 s and 40 s exclusion, exclusion mass window ±7 ppm. MS scans were saved in profile mode while MSMS scans were saved in centroid mode.

Raw files from the orbitrap were processed with MaxQuant (version 1.5.5.1) (http://maxquant.org) (Tyanova et al., 2016). The searches were performed using the Andromeda search engine in MaxQuant on a custom database containing the Avena sequences available from Uniprot augmented with the full complement of ~100 unique UGT-like sequences identified from our oat root tip transcriptome database (Kemen et al., 2014) together with the MaxQuant contaminants database using trypsin/P with 2 missed cleavages, carbamidomethylation (C) as fixed and oxidation (M), acetylation (protein N-terminus), and deamidation (N,Q) as variable modifications. Mass tolerances were 4.5 ppm for precursor ions and 0.5 Da for

fragment ions. Three biological replicates for each of the samples from root tips and the elongation zone were analyzed quantitatively in MaxQuant using the LFQ option.

Gene expression analysis. Expression of *UGT* genes was analyzed by reverse transcription-PCR (RT-PCR). cDNA was generated from mRNA of 3-day-old seedlings for the whole root (WR), root tip (RT; terminal 0.2 cm of the root), root elongation zone (EZ; from 0.2 cm to the first root hair) and young leaves (L). Transcript levels of the housekeeping gene encoding glyceraldehyde-3-phosphate dehydrogenase (*GAPDH*) were used to normalize the cDNA libraries over the 4 tissues. The previously characterized avenacin biosynthetic gene *AsUGT74H5* (*Sad10*) (Owatworakit et al., 2012) was included as a control. Gene-specific primers used for PCR amplification are listed in Supplemental Table 8.

Cloning of the AsUGT coding sequences. Gateway technology (Invitrogen) was used to make UGT expression constructs. The coding sequences (CDSs) including stop codons of *A. strigosa* UGTs were amplified by PCR with a two-step method from root tip cDNA. The first step consisted of specific amplification of full-length coding sequences with gene-specific primers harbouring partial AttB adapters at their 5' ends (see Supplemental Table 8 for primer sequences). The second step involved attachment of full AttB sites at each extremity of the CDS. Amplified fragments were purified using QIAquick PCR Purification Kit (Qiagen). Purified CDSs were then transferred into the pDONR207 vector using BP clonase II enzyme mix (Invitrogen) according to the manufacturer's instructions. Sequence-verified coding sequences were then transferred by the LR clonase II reaction into pH9GW (Invitrogen), a Gateway-compatible variant of pET-28 encoding nine N-terminal histidines (O'Maille et al., 2008).

Expression of recombinant UGTs in *Escherichia coli*. The *E. coli* Rosetta 2 strain DE3 (Novagen) was transformed with the expression vectors following the manufacturer's instructions. Selected transformants were cultured in liquid Lysogeny Broth (LB) media under kanamycin/chloramphenicol (100 μg/mL and 35 μg/mL respectively) selection overnight at 37°C. Pre-cultures were diluted 100-fold into fresh medium to initiate the cultures for induction. Production of recombinant enzymes was induced at 16°C overnight with 0.1 mM of isopropyl β-D-1-thiogalactopyranoside (IPTG) after 30 min of acclimation, and bacterial cells harvested by centrifugation at 4000 g for 10 min. Pellets were lysed enzymatically by

resuspension and incubation at room temperature for 30 min in lysis buffer (50 mM TRIS pH 7.5, 300 mM NaCl, 20 mM imidazol, 5% glycerol, 1% Tween 20 (Sigma), 10 mM β-mercaptoethanol, EDTA free protease inhibitor (Roche), 1 mg/ml lysozyme (Lysozyme human, Sigma)). DNAse treatment was performed at room temperature for 15 min using deoxyribonuclease I from bovine pancreas (Sigma). Sonication of the lysate was performed on ice (3 x 10 s, amplitude 16; Soniprep 150 Plus, MSE). Soluble fractions were then harvested by centrifugation (21,000 g, 4°C, 20 min) and filtered through 0.22 µm filters (Millipore).

For preliminary assays of the oat UGT candidates, the soluble protein fraction was enriched for His-tagged recombinant enzymes using nickel-charged resin (Ni-NTA agarose resin, Qiagen). Ni-NTA resin (300 mL) pre-equilibrated with buffer A (300 mM NaCl, 50 mM TRIS-HCl pH 7.5, 20 mM imidazol, 5% glycerol) was incubated 30 min at 4°C with the protein extract. The resin was washed 3 times with 500 µL buffer A and eluted with 300 µL buffer B (300 mM NaCl, 50 mM TRIS-HCl pH 7.8, 500 mM Imidazol, 5% glycerol). Protein concentrations were estimated from Coomassie-stained SDS-PAGE gels relative to a BSA standard. Quantification of recombinant proteins was performed by densitometric analysis using ImageJ. Alternatively, for enzymatic assays performed with deglycosylated avenacin A-1 (Figure 8B), recombinant UGTs were purified by ion metal affinity chromatography (IMAC) with an ÄKTA purifier apparatus (GE Healthcare) using a nickel-loaded HiTRAP IMAC FF 1 mL column (GE Healthcare) with a flow rate of 0.5 mL/min. The column was pre-equilibrated with buffer A prior to loading with protein extract. Unbound proteins were eluted with buffer A (0-16 min), and a linear gradient of 0-60% buffer B was then applied to the system over 30 min. Fractions containing recombinant enzyme (monitored by UV absorbance at 280 nm) were pooled and concentrated using a 10 kDa centrifugal filter (Amicon, Ultra-4, Sigma). Protein purity was estimated by electrophoresis and protein concentrations were determined using the Bradford method with a BSA standard curve (Bradford, 1976). Samples were aliquoted and flash-frozen in liquid nitrogen prior to storage at -80°C.

Trichlorophenol glycosylation assays. Reactions were carried out in a total volume of 75 µL, composed of 100 mM TRIS-HCl pH 7, 100 µM 2,4,5-trichlorophenol (TCP) and 200 µM uridine diphospho sugars [UDP-α-D-glucose, UDP-α-D-galactose or UDP-β-L-arabinopyranose (see Supplemental Table 7 for suppliers). Reactions

were initiated by addition of 1 µg of enriched recombinant enzyme to pre-warmed reaction mixes and incubated overnight at 28°C before stopping with 3.5 µL trichloroacetic acid (6.1 N). Proteins were precipitated by centrifugation at 21,000 g for 10 min at 4°C. Supernatants were stored at -20°C prior to analysis by HPLC-UV (method A, see Triterpenoids chromatographic analysis section).

Glycosylation assays using different triterpenoid acceptors. Reactions (50 µL) comprised 100 mM TRIS-HCl pH 7.5, 200 µM of triterpenoid (see Supplemental Table 7 for suppliers) and 500 µM uridine diphospho sugars [UDP-α-D-glucose (UDP-Glc), UDP-α-D-galactose (UDP-Gal) or UDP-β-L-arabinopyranose (UDP-Ara); see Supplemental Table 7 for suppliers]. Reactions were initiated by addition of 1 µg of enriched recombinant enzyme to the pre-warmed reaction mix and incubated overnight at 25°C with shaking at 300 rpm. Reactions were stopped by partitioning twice the sample in 100 µL ethyl acetate. The organic phase was dried under N_2 flux and resuspended in 20 µL methanol prior to analysis.

Thin Layer Chromatography (TLC) plates were spotted with 10 µL of methanolic sample and pre-run 3 times in 100% methanol 0.5 cm above the loading line, prior to elution with dichloromethane:methanol:H_2O (80:19:1; v:v:v). They were then sprayed with methanol:sulfuric acid (9:1) and heated to 130°C for 2-3 min until coloration appeared. Photographs were taken under UV illumination at 365 nm. The organic phase was dried under N_2 flux and resuspended in 20 µL methanol for analysis.

Hydrolysis and partial reglycosylation of avenacin A-1. Purified avenacin A-1 (Supplemental Table 7) was hydrolyzed in 1 M HCl for 15 min at 99 °C with shaking at 1400 rpm. The preparation was then cooled on ice and buffered with 1:1 (v:v) unequilibrated TRIS 1 M. The hydrolyzed sample was extracted twice by ethyl acetate, and the combined organic extracts were dried under N_2 flux and resuspended in dimethyl sulfoxide. The resulting hydrolyzed avenacin A-1 (approx. 100 µM in 50 µL reaction volume) was incubated with 500 µM UDP-Ara and 2 µg purified recombinant AsUGT99D1 in 50 mM TRIS-HCl pH 7.5 with 0.5 mM methyl-β-cyclodextrin. After 30 min incubation at 25 °C the reaction was stopped by addition of 2 µL trichloroacetic acid 6.1 N. The precipitated protein was removed by centrifugation at 21,000 g for 10 min at 4°C. The supernatant was diluted with

methanol (50% final volume) before analysis by LC-MS with fluorescence detection (method B see Triterpenoids chromatographic analysis section).

Transient expression in *Nicotiana benthamiana*. UGT CDSs were cloned into pEAQ-*HT*-DEST1 (Sainsbury et al., 2009) via an LR clonase II reaction following the manufacturer's instruction (Invitrogen). Strain culture and agroinfiltrations were performed following previously published methods (Reed et al., 2017). Briefly, expression constructs were introduced into *Agrobacterium tumefaciens* and infiltrated into *N. benthamiana* leaves. Co-expression of combinations of genes was achieved by mixing equal volumes of *A. tumefaciens* strains harboring different expression constructs (previously diluted down to 0.8 OD_{600nm}). An *A. tumefaciens* strain containing a GFP expression construct was used as a control and also co-infiltrated in mixtures as a 'blank' as appropriate to ensure comparable bacterial densities between infiltrations.

Metabolite extraction of *N. benthamiana* leaves. Leaves were harvested 6 days after agro-infiltration and freeze-dried. Freeze-dried leaf material (20 mg) was ground twice at 20 $c.s^{-1}$ for 30 s (TissueLyser, Qiagen). Extractions were carried out in 1 mL 80% methanol with 20 µg of digitoxin (internal standard; Sigma) for 20 min at 90°C, with shaking at 1400 rpm (Thermomixer Comfort, Eppendorf). Samples were centrifuged at 10,000 g for 5 min and 0.8 mL of the supernatant partitioned twice with 0.3 mL of hexane. The aqueous phase was dried *in vacuo* (EZ-2 Series Evaporator, Genevac). Dried material was resuspended in 0.5 mL distilled water and partitioned twice with 0.5 ml of ethyl acetate. The organic phase was dried *in vacuo* and resuspended in 150 µL of methanol followed by filtration (0.2 µm, Spin-X, Costar). Filtered samples were transferred to glass vials and 50 µL of water added. Samples were analyzed by HPLC-CAD following method C (see Triterpenoids chromatographic analysis section).

Purification and structure determination of 12,13-epoxy-16-hydroxy-β-amyrin 3-*O*-arabinoside (EpHβA-Ara). Agro-infiltration of *N. benthamiana* leaves for co-expression of SAD1, SAD2 and UGT99D1 was carried out by vacuum infiltration of 44 *N. benthamiana* plants following published methods (Reed et al., 2017). The plants were harvested 6 days later and the leaves lyophilized. Dried leaf material was ground to a powder using a mortar and pestle and processed by pressurized extraction as described previously (Reed et al., 2017). The extraction method

743 consisted of an initial hexane cycle (5 min pressure holding at 130 bars followed by 3
744 min discharge, extraction cells being heated at 90°C) to remove chlorophylls and
745 apolar pigments. The following 5 cycles were carried out using ethyl acetate and
746 were used for further purification.
747 The crude extract was dried by rotary evaporation before resuspension in 80%
748 aqueous methanol. The methanolic extract was then partitioned three times in n-
749 hexane (1:1) until most of the remaining chlorophyll had been removed. The
750 resulting methanolic sample was dried by rotary evaporation together with
751 diatomaceous earth to allow dry-loading of the flash chromatography column (Celite
752 545 AW, Sigma).

753 Purification was performed using an Isolera One (Biotage) automatic flash
754 purification system. The crude solid was subjected to normal phase flash
755 chromatography (column SNAP KP/Sil 30 g, Biotage). The mobile phase was
756 dichloromethane as solvent A and methanol as solvent B. After an initial isocratic
757 phase with 4% B [5 column volumes (CV)], a gradient was set from 4 to 25% B over
758 40 CV. The fractions containing the EpHβA-Ara were identified by TLC, pooled and
759 then dried down by rotary evaporation together with diatomaceous earth. The
760 resulting solid was subjected to reverse phase flash chromatography (SNAP C_{18}
761 column 12 g, Biotage). The mobile phase was water as solvent A and methanol as
762 solvent B. After an initial isocratic phase with 70% B (3 CV), a gradient was set from
763 70 to 90% B over 20 CV. The fractions containing EpHβA-Ara were identified by TLC
764 and pooled prior to rotary evaporation down to 10 mL. A precipitate was observed in
765 the resulting aqueous sample at 4°C. EpHβA-Ara was pelleted by centrifugation at
766 4000 g for 15 min.

767 NMR spectra were recorded in Fourier transform mode at a nominal frequency of
768 400 MHz for ^{1}H NMR, and 100 MHz for ^{13}C NMR, using deuterated methanol.
769 Chemical shifts were recorded in ppm and referenced to an internal TMS standard.
770 Multiplicities are described as, s = singlet, d = doublet, dd; coupling constants are
771 reported in Hertz as observed and not corrected for second order effects. Where
772 signals overlap ^{1}H δ is reported as the center of the respective HSQC crosspeak
773 (see Supplemental Figure 4).

774 **Characterization of the *aat1* (#807) mutant.** The *AsAAT1* gene was sequenced in
775 47 uncharacterized sodium azide-generated avenacin-deficient mutants

(Papadopoulou et al., 1999; Qi et al., 2006). Genomic DNA was extracted by the Genotyping Scientific Service of the John Innes Centre using an in-house extraction method. PCR amplification of *AsAAT1* full-length CDS (see Supplemental Table 8 for primer sequences) was sequenced (Eurofins), and sequences searched for Single Nucleotide Polymorphisms (SNPs) using CLCbio software (Qiagen).

For analysis of segregating progeny, root tips were harvested from 3-day-old seedlings of F_2 progeny from a cross between the avenacin-deficient mutant #807 and the *A. strigosa* S75 wild type (Papadopoulou et al., 1999), incubated in methanol at 50°C for 15 min with shaking at 1400 rpm, and then put on ice. The methanolic extract was transferred to a new tube, dried under N_2 flux, and resuspended in 50 uL of methanol. Aliquots (5 uL) of each sample were loaded onto TLC plates. Chromatography was carried out using dichloromethane:methanol:H_2O (80:19:1; v:v:v) and the TLCs examined under UV illumination (365 nm). In parallel, genomic DNA was extracted by the Genotyping Scientific Service from the leaves of the same seedlings 10 days after germination [seedlings were grown on distilled water agar after root tip harvesting as previously described (Papadopoulou et al., 1999)]. A 533 bp region spanning the region of the single nucleotide mutation detected in the *AsAAT1* gene of mutant #807 (753G→A) was amplified by PCR for each seedling and sequenced (see Supplemental Table 8 for primers).

Metabolite analysis of oat root extracts. Root tips (5 mg) were harvested from 3-day-old seedlings of wild-type *A. strigosa* and the avenacin-deficient *A. strigosa* mutant #807. Root material was ground using a homogenizer (2010 Geno/Grinder, SPEX SamplePrep) and extracted with methanol following the method described for analysis of triterpenoid glycosides in *N. benthamiana* leaf extracts, detailed above. Filtered methanolic samples were diluted three-fold in 50% methanol and analyzed by LC-MS-CAD-fluorescence (method D, see Triterpenoids chromatographic analysis section).

Pathogenicity tests. Pathogenicity tests to assess root infection with the fungal pathogen *Gaeumannomyces graminis* var. *tritici* isolate T5 were carried out as described previously (Papadopoulou et al., 1999). Seedlings were scored for lesions on the roots following 3 weeks incubation using a 7-point scale.

Linkage analysis. *Avena atlantica* accession Cc7277 (IBERS collection, Aberystwyth University) was sequenced by Illumina technology to approximately 38-fold coverage with a number of paired end and mate pair libraries. Assembled contigs were then mapped by survey sequencing of recombinant inbred lines from a cross between Cc7277 and *A. strigosa* accession Cc7651 (IBERS) (Vickerstaff and Langdon, unpublished). Annotations of contigs linked to the previously identified avenacin biosynthetic genes were used to identify potential UGT candidate genes.

Enzyme assays with recombinant GmSSAT1.

Recombinant GmSSAT1 and UGT73F2: The coding sequences of the soybean candidate UGT GmSSAT1 and the characterized *G. max* UGT73F2, which glucosylates the nonacetylated saponin A0-ag (Sayama et al., 2012) were synthesized commercially (IDT). These sequences were flanked with AttB adapters, allowing subsequent transfer into pH9GW using Gateway technology as described earlier. Recombinant GmSSAT1 was expressed in *E. coli* Rosetta 2 strain DE3 (Novagen) and purified as described in the main text.

Enzyme assays were carried out in 100 µL reaction volumes consisting of 50 mM TRIS-HCl pH 7.5, 100 µM of soyasaponin I and 300 µM uridine diphospho sugars (UDP-α-D-glucose, UDP-α-D-galactose or UDP-β-L-arabinopyranose; see Supplemental Table 7). Reactions were initiated by addition of 1 µg of enriched recombinant enzyme preparation into the pre-warmed samples and incubated at 25°C. After 40, 80 and 200 min, 30 µL of reaction mixture was stopped by addition of methanol (50% final concentration). Assays for glucosylation of the GmSSAT1 product by recombinant UGT73F2 were conducted similarly, after semi-preparative purification of soyasaponin I arabinoside (see below). Samples were analyzed by HPLC-MS-CAD using method D (see Triterpenoids chromatographic analysis section) with modified gradients: 25-46 % [B] over 9.5 min (for GmSSAT1 assays) and 20-46 % [B] over 19.5 min (for UGT73F2 assays). Reactions products were also analysed by HR-MS following method E (see Triterpenoids chromatographic analysis section).

Purification of soyasaponin I arabinoside: Semi-preparative HPLC purification of soyasaponin I arabinoside (SSI-Ara) was carried out with an UltiMate 3000 HPLC system (Dionex) combined with a Corona Veo RS Charged Aerosol Detector (CAD) using a Kinetex column 2.6 µm XB-C18 100 Å, 50 x 2.1 mm (Phenomenex).

GmSSAT1 was incubated with 60 nmoles of soyasaponin I in the presence of excess UDP-Ara until completion. The reaction products were fractionated using a linear gradient (25-46% of acetonitrile:water). Fractions containing SSI-Ara were dried and purity assessed by CAD-HPLC (method D, see Triterpenoids chromatographic analysis section). The purity was comparable to that of commercial soyasaponin I (Chengdu Biopurify Phytochemicals Ltd.; purity >98%).

Structural modelling of AsAAT1. A homology model was generated with I-TASSER (Yang et al., 2015) using the crystal structure of *Medicago truncatula* UGT71G1 complexed with UDP-Glc as a template (PDB entry: 2ACW) (Shao et al., 2005). This homology model contained a strained loop comprising residues Trp396 to Ser402 due to a 2-residue insertion relative to the template. To identify the most likely conformation for this loop, 20 loop models were generated using the MODELLER (Sali and Blundell, 1993) plugin to Chimera (Pettersen et al., 2004). The six loop conformations with the best scores in terms of zDOPE, estimated RMSD and estimated overlap were used to generate models for the structure of the complex with UDP-Ara, based on the conformation of UDP-Glc found in PDB entry 2ACW (Shao et al., 2005). The resulting draft-docked complexes were relaxed using the molecular dynamics program GROMACS (Van Der Spoel et al., 2005) and the force field 53a6 (Oostenbrink et al., 2004). The models were solvated in a cubic periodic box of SPC 3-site water molecules and subjected to 104 steps of energy minimization. The necessary parameters for UDP-Ara were based on those available for uridine, ATP and glucose in the 53a6 forcefield. Following this step, the optimal model was selected for analysis based on having the best QMEAN score (Benkert et al., 2008) and no Ramanchandran or rotamer outliers in the remodelled loop according to the structure validation service, MolProbity (Chen et al., 2010).

Purification of hydrolysed avenacin A-1. Hydrolysis of purified avenacin A-1 (483 µg, Supplemental Table 7) was scaled up using the method described previously (*i.e.*, partial re-glycosylation of avenacin A-1). The entire sample was directly subjected to reverse phase flash chromatography (SNAP C_{18} column 12 g, Biotage). Elution was performed with a linear gradient from 65 to 72% methanol:water over 55 CV. Elution of hydrolysed avenacin A-1 was monitored by absorbance at 365 nm. Fluorescent fractions were collected, dried via rotary evaporation, and subjected to normal phase flash chromatography (column SNAP KP/Sil 30 g, Biotage). The

mobile phase was dichloromethane as solvent A and methanol as solvent B. After an initial isocratic phase with 5% B (5 CV), a gradient was set from 5 to 11% B over 40 CV. Fluorescent fractions were pooled and dried. No impurities were detected by HPLC-CAD-fluorescence analysis. Absolute quantification was carried out by HPLC-fluorescence using an avenacin A-1 standard. A total of 208 µg of hydrolysed product was recovered and dissolved in DMSO as a 5 mM stock solution for use in enzyme assays.

Mutagenesis of AsAAT1. Site-directed mutagenesis was performed by PCR amplification using the expression vector pH9GW-AsAAT1 as the template and the mutated complementary sequences as primers (Supplemental Table 8). Mutagenized genes were cloned into the entry vector pDONR207, transferred back into the pH9GW expression vector, and transformed into *E. coli* BL21 Rosetta. Recombinant enzymes were purified via IMAC using an ÄKTA purifier apparatus and quantified with the Bradford method as described above.

In vitro analysis of the AsAAT1 wild-type enzyme and mutant variants. Wild-type and mutagenized AsAAT1 enzymes were expressed and purified as described above (Supplemental Figure 7A). Optimal catalytic conditions for AsAAT1 were observed at pH 6.5. Reactions were carried out in 55 µL volumes at 25°C and sampled under steady-state conditions by transferring 10 µL reaction mix into 55 µL ice cold 10% TCA to stop the reaction. Sugar donor mix (10 µL) containing 5 µM UDP-Ara, UDP-Glc, UDP-Xyl or UDP-Gal was added to pre-warmed enzyme. The latter was composed of 30 µM deglycosylated avenacin A-1 dissolved in 0.5 mM methyl-β-cyclodextrin (substrate inhibition was observed with acceptor concentrations of ≥ 30 µM). Reactions were carried out in 50 mM TRIS-HCl pH 6.5 with 0.3 µg of recombinant enzyme. Precipitated protein was removed by centrifugation at 21,000 g for 10 min at 4°C and supernatants stored at ˉ20°C prior to analysis by HPLC-fluorescence (method F, see Triterpenoids chromatographic analysis section).

Triterpenoids chromatographic analysis

All analytical liquid chromatography methods were designed with a flow rate of 0.3 $mL.min^{-1}$ and a Kinetex column 2.6 µm XB-C18 100 Å, 50 x 2.1 mm (Phenomenex).

Solvent A: [H_2O + 0.1 % formic acid (FA)] Solvent B: [acetonitrile (CH_3CN) + 0.1% FA].

Method A - HPLC-UV analysis of TCP glycosylation assays: Instrument: Dionex UltiMate 3000. Injection volume: 15 µL. Gradient: 20% [B] from 0 to 1.5 min, 20% to 50% [B] from 1.5 to 16 min, 50% to 95% [B] from 16 to 16.5 min, 95% [B] from 16.5 to 18.5 min, 95% to 20% [B] from 18.5 to 20 min. Detection: UV 205 nm.

Method B – Analysis of avenacin A-1 reglycosylation assay using LCMS-fluorescence: Instrument: Prominence HPLC system, RF-20Axs fluorescence detector, single quadrupole mass spectrometer LCMS-2020 (Shimadzu). Injection volume: 5 µL. Gradient: 35% [B] from 0 to 2 min, 35% to 50% [B] from 2 to 12 min, 50% to 95% [B] from 12 to 12.5 min, 95% [B] from 12.5 to 14 min, 95% to 35% [B] from 14 to 14.1 min, 35% [B] from 14.1 to 15 min. Detection: fluorescence (Ex 353 nm/Em 441 nm), MS (dual ESI/APCI ionization, DL temp 250°C, neb gas flow 15 L.min-1, heat block temp 400°C, spray voltage Pos 4.5 kV, Neg -3.5 kV).

Method C – HPLC-CAD analysis of N. benthamiana methanolic extracts: Instrument: UltiMate 3000 HPLC system, Corona Veo RS Charged Aerosol Detector (CAD) (Dionex). Injection volume: 15 µL. Gradient: 25% [B] from 0 to 1.5 min, 25% to 58% [B] from 1.5 to 16 min, 58% to 95% [B] from 16 to 16.5 min, 95% [B] from 16.5 to 18.5 min, 95% to 25% [B] from 18.5 to 19 min, 35% [B] from 19 to 20 min. Detection: charged aerosol (data collection rate 10 Hz, filter constant 3.6 s, evaporator temp. 35°C, ion trap voltage 20.5 V).

Method D – Metabolites analysis of oat root tips using LCMS-CAD-fluorescence: Instrument: Prominence HPLC system, RF-20Axs fluorescence detector (Shimadzu), single quadrupole mass spectrometer LCMS-2020 (Shimadzu), Corona Veo RS CAD (Dionex). Injection volume: 10 µL. Gradient: 20% [B] from 0 to 3 min, 20% to 60% [B] from 3 to 28 min, 60% to 95% [B] from 28 to 30 min, 95% [B] from 30 to 33 min, 95% to 20% [B] from 33 to 34 min, 20% [B] from 34 to 35 min. Detection: fluorescence and charged aerosol (settings identical to previous methods).

Method E – HRMS analysis of in vitro reaction with recombinant soybean enzymes: Instrument: Prominence HPLC system, IT-TOF mass spectrometer

(Shimadzu). Injection volume: 5 µL. Gradient: 20% [B] from 0 to 2 min, 20% to 46% [B] from 2 to 16.5 min, 46% to 95% [B] from 16.5 to 17 min, 95% [B] from 17 to 18.5 min, 95% to 20% [B] from 18.5 to 19 min, 20% [B] from 19 to 20 min. Detection: Neg. ESI ionization (capillary temp. 250°C, nebulizing gas 1.5 L.min-1, heat block temp. 300°C, spray voltage -3.5 kV. Energy/collision gas MS2 50%, MS3 75%).

Method F – HPLC-fluorescence analysis of enzymatic assay with deglycosylated avenacin A-1 as substrate: Instrument: Prominence HPLC system, RF-20Axs fluorescence detector (Shimadzu). Injection volume: 7 µL. Gradient: 40% [B] from 0 to 2 min, 40% to 50% [B] from 2 to 6 min, 50% to 95% [B] from 6.5 to 7 min, 95% [B] from 7 to 7.5 min, 95% to 20% [B] from 7.5 to 8 min, 20% [B] from 8 to 9 min. Detection: fluorescence (Ex 353 nm/Em 441 nm).

Gas chromatography

Sample preparation and GC-MS analysis was performed as described previously (Reed et al., 2017). Briefly, approximately 5 mg of dried agro-infiltrated leaf material was saponified in alkaline conditions. Hexane partitioning was used to remove saponified pigments. The unsaponifiable aqueous fraction was derivatized with 1-(trimethylsilyl)imidazole (Sigma) and analyzed by GC-MS. Coprostan-3-ol (Sigma) was used as an internal standard (final concentration of 10 µg/mL).

Accession Numbers

Sequence data from this article can be found in the GenBank database under the following accession numbers: AsAAT1, MH244526; GmSSAT1, XM_003532226. The *A. strigosa* sequences used in phylogeny reconstructions are available in Supplemental Table 3.

Supplemental Data

Supplemental Figure 1. Proteomic analysis of *A. strigosa* root samples.

Supplemental Figure 2. TLC analysis of AsUGT99D1 activity towards the SAD2 product 12,13-epoxy-16-hydroxy-ß-amyrin (EpHβA).

966 **Supplemental Figure 3.** Purification of AsUGT99D1 product obtained by transient
967 co-expression of AsUGT99D1, SAD1 and SAD2.

968 **Supplemental Figure 4.** ^{1}H and ^{13}C NMR of the major product generated by co-
969 expression of SAD1, SAD2 and UGT99D1 in *N. benthamiana*.

970 **Supplemental Figure 5.** Characterization of avenacin-deficient oat mutant #807.

971 **Supplemental Figure 6.** HR-MS analysis of the products of recombinant soybean
972 UGTs GmSSAT1 and UGT73F2 and expression patterns of GmSSAT1, UGT73F2
973 and other genes involved in soyasaponin biosynthesis.

974 **Supplemental Figure 7.** Mutation of AsAAT1 and comparison of wild-type and
975 mutant enzymes by transient plant expression and in In vitro assays.

976 **Supplemental Table 1.** Characterized triterpene glycosyltransferases

977 **Supplemental Table 2.** *A. thaliana* UGT protein sequences used in tBLASTn
978 analysis

979 **Supplemental Table 3.** *A. strigosa* UGT sequences found by transcriptome mining
980 and used in subsequent analysis

981 **Supplemental Table 4.** UGT amino acid sequences used for phylogenetic analysis

982 **Supplemental Table 5.** Mapping of candidate avenacin glycosyltransferase genes.

983 **Supplemental Table 6.** Candidate soybean arabinosyltransferases identified by
984 genome mining

985 **Supplemental Table 7.** Chemicals and suppliers

986 **Supplemental Table 8.** Primers

987 **Supplemental Data set 1.** Alignment of oat UGTs as well as selected characterized
988 enzymes from the GT1 family used for the phylogenetic reconstruction displayed in
989 Figure 2A.

990 **Supplemental Data set 2.** Sequence of the scaffold containing *AsAAT1* in *A.*
991 *atlantica*.

992 **Supplemental Data set 3.** Alignment of selected group D enzymes used for the
993 phylogenetic reconstruction displayed in Figure 6B.

994

995

ACKNOWLEDGMENTS

We thank Lionel Hill and Paul Brett of John Innes Metabolite Services for advice on metabolite analysis, and Andrew Davis for photography. This work was supported by Innovate UK Industrial Biotechnology Catalyst award no.48489-341232 (A.O., T. Louveau), the joint Engineering and Physical Sciences Research Council/ Biotechnological and Biological Sciences Research Council (BBSRC)-funded OpenPlant Synthetic Biology Research Centre grant BB/L014130/1 (M.S., A.O.), BBSRC grant BB/K005952/1 (A.L.), BBSRC Doctoral Training Programme studentship awards to H.P. and A. Orme, the BBSRC-funded Institute Strategic Programme Grant ‘Molecules from Nature’ (BB/P012523/1) and the John Innes Foundation and BBSRC award BB/H009582/1 LINK (T. Langdon).

AUTHOR CONTRIBUTIONS

T. Louveau, A. Orme, H.P., M.J.S., R.M, G.S., A.L. and R.J.V. performed the research. M.R., A.M.H., T.L and R.A.F. advised on crucial aspects of the research and revised the article. T. Louveau and A.O. designed the research and wrote the article.

Figure 1. Triterpene glycoside structures and avenacin biosynthesis. (**A)** Avenacins: antifungal defense compounds from oat. (**B**) Soyasaponin Ab, a triterpene glycoside associated with bitterness and anti-feedant activity in soybean. (**C**) Current understanding of the avenacin biosynthetic pathway. The major avenacin, A-1, is synthesised from the linear isoprenoid precursor 2,3-oxidosqualene. 2,3-Oxidosqualene is cyclized by the triterpene synthase AsbAS1 (SAD1) to the pentacyclic triterpene scaffold β-amyrin (Haralampidis et al., 2001). β-Amyrin is then oxidized to 12,13β-epoxy-16β-hydroxy-β-amyrin (EpHβA) by the cytochrome P450 enzyme AsCYP51H10 (SAD2) (Geisler et al., 2013). Subsequent, as-yet uncharacterized modifications involve a series of further oxygenations and addition of a branched trisaccharide moiety at the C-3 position, initiated by introduction of an L-arabinose. Acylation at the C-21 position is carried out by the serine carboxypeptidase-like acyl transferase AsSCPL1 (SAD7). The acyl donor used by AsSCPL1 is *N*-methyl anthranilate glucoside, which is generated by the methyl transferase AsMT1 and the glucosyl transferase AsUGT74H5 (SAD10) (Mugford et al., 2009; Owatworakit et al., 2012; Mugford et al., 2013).

Figure 2. Mining for candidate avenacin glycosyltransferase genes. (**A**) Phylogenetic tree of UGTs expressed in *A. strigosa* root tips (red) (listed in Supplemental Table 3). Characterized triterpenoid glycosyltransferases from other plant species (blue) and other biochemically characterized plant UGTs (black) are also included (listed in Supplemental Table 4). The UGT groups are as defined by Ross et al. (2001). Some of the most common groups of enzyme activities are indicated. The tree was constructed using the Neighbour Joining method with 1000 bootstrap replicates (% support for branch points shown). The scale bar indicates 0.1 substitutions per site at the amino acid level. The alignment file is available as Supplemental Data set 1. (**B**) Expression profiles of selected oat UGT genes (RT-PCR). Tissues were collected from 3-day-old *A. strigosa* seedlings. The characterized avenacin biosynthetic gene *AsUGT74H5* (*Sad10*) and the glyceraldehyde 3-phosphate dehydrogenase (*GAPDH*) housekeeping gene are included as controls.

Figure 3. Biochemical characterization of candidate oat UGTs.

(**A**) Evaluation of sugar donor specificity of recombinant oat UGTs using the universal acceptor 2,4,5-trichlorophenol (TCP). Relative activities with different sugar nucleotide donors are shown. Conversion of TCP to TCP glycoside was monitored by spectrophotometry at 405 nm. The previously characterized oat *N*-methyl anthranilate glucosyltransferase AsUGT74H5 (SAD10) and *A. thaliana* flavonoid arabinosyltransferase UGT78D3 were included as controls. Values are means of three biological replicates; error bars represent standard deviations. (**B**) LC-MS profiles for avenacin A-1 (left), deglycosylated avenacin A-1 (middle), and the product generated by incubation of deglycosylated avenacin A-1 with AsUGT99D1 (right) (detection by fluorescence; excitation and emission wavelengths 353 and 441 nm, respectively). The hydrolyzed avenacin product is shown with an intact 12,13-epoxide (*), but this epoxide may have rearranged to a ketone under the acidic hydrolysis conditions resulting in deglycosylated 12-oxo-avenacin A-1, as observed previously (Geisler et al., 2013).

Figure 4. Transient expression of AsAAT1 in *Nicotiana benthamiana*.
(A) GC-MS analysis of extracts from agro-infiltrated *N. benthamiana* leaves. Comparison of the metabolite profiles of leaves expressing SAD1 and SAD2 (red) or SAD1, SAD2 and UGT99D1 (blue). EpHβA , identified previously as the co-expression product of SAD1 and SAD2 is indicated by an arrow (Geisler et al., 2013). The upper chromatogram consists of a control from leaves expressing GFP only (black). (**B**) HPLC with charged aerosol detection (CAD) chromatograms of extracts from *N. benthamiana* leaves expressing UGT99D1 alone (green), SAD1 and UGT99D1 (grey) and SAD1, SAD2 and UGT99D1 together (blue). The new compound that accumulated in the latter (t_R 12.0 min) is indicated by an asterisk. This compound was not detected when UGT99D1 was expressed on its own or with SAD1. The internal standard (IS) was digitoxin (1 mg/g of dwt). (**C**) Structure of the UGT99D1 product (see Supplemental Figure 4 for NMR assignment).

Figure 5. Biochemical analysis of *aat1* mutant and susceptibility to take-all disease.

(**A**) HPLC-CAD analysis of methanolic root extracts from seedlings of the *A. strigosa* wild-type accession and avenacin-deficient mutant line #807 (*aat1*). New metabolites detected in the mutant are arrowed and inferred structures are shown based on the corresponding ion chromatograms (Supplemental Figure 5D). (**B**) *aat1* (#807) has enhanced disease susceptibility. Images of representative seedlings of wild-type *A. strigosa* (WT), the *sad1* mutant #610 (Haralampidis et al., 2001), and the *aat1* mutant (this study) are shown. Seedlings were inoculated with the take-all fungus (*G. graminis* var. *tritici*). The dark lesions on the roots are symptoms of infection and are indicated by arrows.

Figure 6. An arabinosyltransferase from soybean.

(**A**) Alignment of the amino acid sequences of the oat, soybean and *A. thaliana* arabinosyltransferases with the closest characterized glucosyltransferases in the region of the PSPG motif and the N5 loop. The histidine residue that is conserved in the arabinosyltransferases is shown in red. P154 and the two additional amino acids IG of AsAAT1 are also highlighted. (**B**) Phylogenetic analysis of glycosyltransferases from group D belonging to the UGT73 family. GmSSAT1 and AsAAT1 are indicated in red, and other characterized triterpenoid glycosyltransferases in blue (see Supplemental Table 4 for further details). The tree was constructed using the Neighbour Joining method with 1000 bootstrap replicates (percentage support shown at branch points), and rooted with UGT90A1, an *A. thaliana* UGT from group C. The scale bar indicates 0.1 substitutions per site at the amino acid level. The alignment file is available as Supplemental Data set 3.

Figure 7. Biochemical characterization of GmSSAT1.

(**A**) HPLC-CAD chromatogram of *in vitro* assays performed with recombinant GmSSAT1 and different UDP-sugars. GmSSAT1 was incubated for 40 min at 25°C with 100 µM soyasaponin I (SSI) and 300 µM UDP-sugars. A major product is detected only in the presence of UDP-Ara (*) (see Supplemental Figure 7A for MS analysis). (**B**) HPLC-CAD analysis of reactions in which the previously characterized soyasaponin glucosyltransferase UGT73F2 (Sayama

et al., 2012) was assayed for activity towards the GmSSAT1 product. Recombinant UGT73F2 was incubated overnight with 400 µM UDP-Glc and approximately 100 µM of the GmSSAT1 product SSI-22-*O*-α-L-arabinoside (SSI-Ara). SSI-Ara (t_R: 10.6 min) was completely converted to a new product with a t_R of 8.6 min (asterisked). MS analysis of this product is shown in Supplemental Figure 7B. No product was detected in the absence of UDP-Glc or if the acceptor was replaced by SSI. (**C**) Schematic showing successive glycosylation of soyasaponin I by GmSSAT1 and UGT73F2.

Figure 8. Determinants of sugar donor sugar specificity of AsAAT1.
(**A**) Model of AsAAT1 with bound UDP-Ara (carbons of the arabinose numbered). The protein is represented in green ribbons with the PSPG motif in salmon, including the side chains of highly conserved residues. The His404 and Pro154 residues are shown in magenta. Potential hydrogen bonds are shown with yellow dots, and the distance between P154 and C-5 of UDP-Ara with grey dots The homology model was generated using I-TASSER software (Yang et al., 2015), based on the crystal structure of *Medicago truncatula* UGT71G1 complexed with UDP-Glc (PDB: 2ACW). The loop shown in orange was reconstructed using MODELLER (Sali and Blundell, 1993). UDP-Ara was inserted into the active site and the complex was relaxed for energy minimization using GROMACS. (**B**) Comparison of the glycosylation activity of the AsAAT1 wild-type and mutant enzymes when supplied with each of the four sugar donors (UDP-Ara, UDP-Gal, UDP-Xyl or UDP-Glc). Initial velocities were measured using 30 µM deglycosylated avenacin A-1 as acceptor and 5 µM UDP-sugar donor using five timepoints. The heights of the bars are drawn relative to the highest activity observed for each recombinant enzyme (mean ± SD, n = 3). Activities reported above each bar are in $nM.min^{-1}$. (**C**) HPLC-CAD analysis of extracts from *N. benthamiana* leaves expressing SAD1 and SAD2 together with GFP (black), wild-type AsAAT1 enzyme (blue), AsAAT1-H404Q (green), AsAAT1-P154S (red) and AsAAT1-H404Q-P154S (orange). The top trace (in grey) shows the products of *in vitro* reaction of 12,13β-epoxy-16β-hydroxy-β-amyrin (EpHβA) with the four sugar donors (reactions carried out separately and then pooled) for reference. LC-MS analysis was used to

confirm the identities of the new products (Supplemental Figure 8*C*). The internal standard (IS) is digitoxin (1 mg/g dwt).

Table 1. Candidate avenacin glycosyltransferase genes

***A. strigosa* UGT genes**	**Group**	**Gene expression profiles ***				**Protein level ratio (RT/EZ)†**
		RT	**EZ**	**WR**	**L**	
AsUGT98B4	D	+++	+	++	++	n.d in EZ
AsUGT701A5	D	+++	+	++	-	n.d
AsUGT99C4	D	++	-	+	-	n.d in EZ
AsUGT99D1	D	+++	-	++	-	2.30
AsUGT99B9	D	+++	++	++	++	0.78
AsUGT99A6	D	++	-	++	-	n.d in RT
AsUGT705A4	_	+++	-	++	-	0.77
AsUGT706F7	E	+++	+	++	+	1.34
AsUGT93B16	O	+++	+	+++	+++	1.70
AsUGT74H5	L	+++	-	++	-	5.56

RT, root tip; EZ, elongation zone; WR, whole root; L, leaves.
n.d., not detected
*Gene expression profiles were obtained by RT-PCR (see Figure 2B). "-" indicates an absence of amplification; "+", "++" and "+++"indicate the relative intensity of the amplified fragment on the gel based on the housekeeping gene *GAPDH*.
†Based on proteomic analysis (see Supplemental Figure 1) and displayed as a ratio of protein detected between root tip (RT) and elongation zone (EZ).

Table 2. Segregation ratios for the F_2 progeny from crosses between #807 mutant and *A. strigosa* wild type.

Chemotypes*		χ^2
Wt	Mut	**Wild type : mutant (3:1)**
104	35	0.961 ($P > 0.05$)

*Chemotype analysis was performed by TLC-UV (Supplemental Figure 5C).

References

Achnine, L., Huhman, D.V., Farag, M.A., Sumner, L.W., Blount, J.W., and Dixon, R.A. (2005). Genomics-based selection and functional characterization of triterpene glycosyltransferases from the model legume *Medicago truncatula*. Plant J. **41,** 875-887.

Armah, C.N., Mackie, A.R., Roy, C., Price, K., Osbourn, A.E., Bowyer, P., and Ladha, S. (1999). The membrane-permeabilizing effect of avenacin A-1 involves the reorganization of bilayer cholesterol. Biophys. J. **76,** 281-290.

Augustin, J.M., Kuzina, V., Andersen, S.B., and Bak, S. (2011). Molecular activities, biosynthesis and evolution of triterpenoid saponins. Phytochemistry **72,** 435-457.

Augustin, J.M., Drok, S., Shinoda, T., Sanmiya, K., Nielsen, J.K., Khakimov, B., Olsen, C.E., Hansen, E.H., Kuzina, V., Ekstrom, C.T., Hauser, T., and Bak, S. (2012). UDP-glycosyltransferases from the UGT73C subfamily in *Barbarea vulgaris* catalyze sapogenin 3-*O*-glucosylation in saponin-mediated insect resistance. Plant Physiol. **160,** 1881-1895.

Benkert, P., Tosatto, S.C., and Schomburg, D. (2008). QMEAN: A comprehensive scoring function for model quality assessment. Proteins **71,** 261-277.

Bernard, F.X., Sable, S., Cameron, B., Provost, J., Desnottes, J.F., Crouzet, J., and Blanche, F. (1997). Glycosylated flavones as selective inhibitors of topoisomerase IV. Antimicrob. Agents Chemother. **41,** 992-998.

Bowles, D., Lim, E.K., Poppenberger, B., and Vaistij, F.E. (2006). Glycosyltransferases of lipophilic small molecules. Annu. Rev. Plant Biol. **57,** 567-597.

Bradford, M.M. (1976). A rapid and sensitive method for the quantitation of microgram quantities of protein utilizing the principle of protein-dye binding. Anal. Biochem. **72,** 248-254.

Caputi, L., Lim, E.K., and Bowles, D.J. (2008). Discovery of new biocatalysts for the glycosylation of terpenoid scaffolds. Chemistry **14,** 6656-6662.

Caputi, L., Malnoy, M., Goremykin, V., Nikiforova, S., and Martens, S. (2011). A genome-wide phylogenetic reconstruction of family 1 UDP-glycosyltransferases revealed the expansion of the family during the adaptation of plants to life on land. Plant J. **69,** 1030-1042.

Chen, V.B., Arendall, W.B., 3rd, Headd, J.J., Keedy, D.A., Immormino, R.M., Kapral, G.J., Murray, L.W., Richardson, J.S., and Richardson, D.C. (2010). MolProbity: all-atom structure validation for macromolecular crystallography. Acta Crystallogr D Biol Crystallogr **66,** 12-21.

Dai, L., Liu, C., Zhu, Y., Zhang, J., Men, Y., Zeng, Y., and Sun, Y. (2015). Functional characterization of cucurbitadienol synthase and triterpene glycosyltransferase involved in biosynthesis of mogrosides from *Siraitia grosvenorii*. Plant Cell Physiol. **56,** 1172-1182.

Francis, G., Kerem, Z., Makkar, H.P., and Becker, K. (2002). The biological action of saponins in animal systems: a review. Br J Nutr **88,** 587-605.

Gachon, C.M., Langlois-Meurinne, M., and Saindrenan, P. (2005). Plant secondary metabolism glycosyltransferases: the emerging functional analysis. Trends Plant Sci. **10,** 542-549.

Geisler, K., Hughes, R.K., Sainsbury, F., Lomonossoff, G.P., Rejzek, M., Fairhurst, S., Olsen, C.E., Motawia, M.S., Melton, R.E., Hemmings, A.M., Bak, S., and Osbourn, A. (2013). Biochemical analysis of a multifunctional cytochrome P450 (CYP51) enzyme required for synthesis of antimicrobial triterpenes in plants. Proc Natl Acad Sci U S A **110,** 3360-3367.

Grille, S., Zaslawski, A., Thiele, S., Plat, J., and Warnecke, D. (2010). The functions of steryl glycosides come to those who wait: Recent advances in plants, fungi, bacteria and animals. Prog Lipid Res **49,** 262-288.

Han, S.H., Kim, B.G., Yoon, J.A., Chong, Y., and Ahn, J.H. (2014). Synthesis of flavonoid *O*-pentosides by *Escherichia coli* through engineering of nucleotide sugar pathways and glycosyltransferase. Appl. Environ. Microbiol. **80,** 2754-2762.

Haralampidis, K., Bryan, G., Qi, X., Papadopoulou, K., Bakht, S., Melton, R., and Osbourn, A. (2001). A new class of oxidosqualene cyclases

directs synthesis of antimicrobial phytoprotectants in monocots. Proc Natl Acad Sci U S A **98,** 13431-13436.

Hartley, J.L., Temple, G.F., and Brasch, M.A. (2000). DNA cloning using in vitro site-specific recombination. Genome Res. **10,** 1788-1795.

He, X.Z., Wang, X., and Dixon, R.A. (2006). Mutational analysis of the Medicago glycosyltransferase UGT71G1 reveals residues that control regioselectivity for (iso)flavonoid glycosylation. J. Biol. Chem. **281,** 34441-34447.

Hughes, J., and Hughes, M.A. (1994). Multiple secondary plant product UDP-glucose glucosyltransferase genes expressed in cassava (*Manihot esculenta* Crantz) cotyledons. DNA Seq **5,** 41-49.

Kemen, A.C., Honkanen, S., Melton, R.E., Findlay, K.C., Mugford, S.T., Hayashi, K., Haralampidis, K., Rosser, S.J., and Osbourn, A. (2014). Investigation of triterpene synthesis and regulation in oats reveals a role for beta-amyrin in determining root epidermal cell patterning. Proc Natl Acad Sci U S A **111,** 8679-8684.

Kubo, A., Arai, Y., Nagashima, S., and Yoshikawa, T. (2004). Alteration of sugar donor specificities of plant glycosyltransferases by a single point mutation. Arch Biochem Biophys **429,** 198-203.

Li, Y., Baldauf, S., Lim, E.K., and Bowles, D.J. (2001). Phylogenetic analysis of the UDP-glycosyltransferase multigene family of *Arabidopsis thaliana*. J. Biol. Chem. **276,** 4338-4343.

Liu, Z., Liu, Y., Pu, Z., Wang, J., Zheng, Y., Li, Y., and Wei, Y. (2013). Regulation, evolution, and functionality of flavonoids in cereal crops. Biotechnol. Lett. **35,** 1765-1780.

Mackenzie, P.I., Owens, I.S., Burchell, B., Bock, K.W., Bairoch, A., Belanger, A., Fournel-Gigleux, S., Green, M., Hum, D.W., Iyanagi, T., Lancet, D., Louisot, P., Magdalou, J., Chowdhury, J.R., Ritter, J.K., Schachter, H., Tephly, T.R., Tipton, K.F., and Nebert, D.W. (1997). The UDP glycosyltransferase gene superfamily: recommended nomenclature update based on evolutionary divergence. Pharmacogenetics **7,** 255-269.

Meesapyodsuk, D., Balsevich, J., Reed, D.W., and Covello, P.S. (2007). Saponin biosynthesis in *Saponaria vaccaria*. cDNAs encoding beta-

amyrin synthase and a triterpene carboxylic acid glucosyltransferase. Plant Physiol. **143,** 959-969.

Messner, B., Thulke, O., and Schaffner, A.R. (2003). Arabidopsis glucosyltransferases with activities toward both endogenous and xenobiotic substrates. Planta **217,** 138-146.

Mugford, S.T., Louveau, T., Melton, R., Qi, X., Bakht, S., Hill, L., Tsurushima, T., Honkanen, S., Rosser, S.J., Lomonossoff, G.P., and Osbourn, A. (2013). Modularity of plant metabolic gene clusters: A trio of linked genes that are collectively required for acylation of triterpenes in oat. Plant Cell **25,** 1078–1092.

Mugford, S.T., Qi, X., Bakht, S., Hill, L., Wegel, E., Hughes, R.K., Papadopoulou, K., Melton, R., Philo, M., Sainsbury, F., Lomonossoff, G.P., Roy, A.D., Goss, R.J., and Osbourn, A. (2009). A serine carboxypeptidase-like acyltransferase is required for synthesis of antimicrobial compounds and disease resistance in oats. Plant Cell **21,** 2473-2484.

Mylona, P., Owatworakit, A., Papadopoulou, K., Jenner, H., Qin, B., Findlay, K., Hill, L., Qi, X., Bakht, S., Melton, R., and Osbourn, A. (2008). *Sad3* and *Sad4* are required for saponin biosynthesis and root development in oat. Plant Cell **20,** 201-212.

Naoumkina, M.A., Modolo, L.V., Huhman, D.V., Urbanczyk-Wochniak, E., Tang, Y., Sumner, L.W., and Dixon, R.A. (2010). Genomic and coexpression analyses predict multiple genes involved in triterpene saponin biosynthesis in *Medicago truncatula*. Plant Cell **22,** 850-866.

Noguchi, A., Horikawa, M., Fukui, Y., Fukuchi-Mizutani, M., Iuchi-Okada, A., Ishiguro, M., Kiso, Y., Nakayama, T., and Ono, E. (2009). Local differentiation of sugar donor specificity of flavonoid glycosyltransferase in Lamiales. Plant Cell **21,** 1556-1572.

O'Maille, P.E., Malone, A., Dellas, N., Andes Hess, B., Jr., Smentek, L., Sheehan, I., Greenhagen, B.T., Chappell, J., Manning, G., and Noel, J.P. (2008). Quantitative exploration of the catalytic landscape separating divergent plant sesquiterpene synthases. Nat. Chem. Biol. **4,** 617-623.

Oostenbrink, C., Villa, A., Mark, A.E., and van Gunsteren, W.F. (2004). A biomolecular force field based on the free enthalpy of hydration and solvation: the GROMOS force-field parameter sets 53A5 and 53A6. J Comput Chem **25,** 1656-1676.

Osbourn, A. (1996). Saponins and plant defence - a soap story. Trends Plant Sci. **1,** 4-9.

Osbourn, A., Bowyer, P., Lunness, P., Clarke, B., and Daniels, M. (1995). Fungal pathogens of oat roots and tomato leaves employ closely related enzymes to detoxify different host plant saponins. Mol Plant Microbe Interact **8,** 971-978.

Osmani, S.A., Bak, S., and Moller, B.L. (2009). Substrate specificity of plant UDP-dependent glycosyltransferases predicted from crystal structures and homology modeling. Phytochemistry **70,** 325-347.

Osmani, S.A., Bak, S., Imberty, A., Olsen, C.E., and Moller, B.L. (2008). Catalytic key amino acids and UDP-sugar donor specificity of a plant glucuronosyltransferase, UGT94B1: molecular modeling substantiated by site-specific mutagenesis and biochemical analyses. Plant Physiol. **148,** 1295-1308.

Owatworakit, A., Townsend, B., Louveau, T., Jenner, H., Rejzek, M., Hughes, R.K., Saalbach, G., Qi, X., Bakht, S., Deb Roy, A., Mugford, S.T., Goss, R.J., Field, R.A., and Osbourn, A. (2012). Glycosyltransferases from oat (Avena) implicated in the acylation of avenacins. J. Biol. Chem. **288,** 3696-3704.

Papadopoulou, K., Melton, R.E., Leggett, M., Daniels, M.J., and Osbourn, A.E. (1999). Compromised disease resistance in saponin-deficient plants. Proc Natl Acad Sci U S A **96,** 12923-12928.

Pettersen, E.F., Goddard, T.D., Huang, C.C., Couch, G.S., Greenblatt, D.M., Meng, E.C., and Ferrin, T.E. (2004). UCSF Chimera--a visualization system for exploratory research and analysis. J Comput Chem **25,** 1605-1612.

Piochon, M., Legault, J., Gauthier, C., and Pichette, A. (2009). Synthesis and cytotoxicity evaluation of natural alpha-bisabolol beta-D-fucopyranoside and analogues. Phytochemistry **70,** 228-236.

Qi, X., Bakht, S., Leggett, M., Maxwell, C., Melton, R., and Osbourn, A. (2004). A gene cluster for secondary metabolism in oat: implications for the evolution of metabolic diversity in plants. Proc Natl Acad Sci U S A **101,** 8233-8238.

Qi, X., Bakht, S., Qin, B., Leggett, M., Hemmings, A., Mellon, F., Eagles, J., Werck-Reichhart, D., Schaller, H., Lesot, A., Melton, R., and Osbourn, A. (2006). A different function for a member of an ancient and highly conserved cytochrome P450 family: from essential sterols to plant defense. Proc Natl Acad Sci U S A **103,** 18848-18853.

Qin, B., Eagles, J., Mellon, F.A., Mylona, P., Pena-Rodriguez, L., and Osbourn, A.E. (2010). High throughput screening of mutants of oat that are defective in triterpene synthesis. Phytochemistry **71,** 1245-1252.

Reed, J., Stephenson, M.J., Miettinen, K., Brouwer, B., Leveau, A., Brett, P., Goss, R.J.M., Goossens, A., O'Connell, M.A., and Osbourn, A. (2017). A translational synthetic biology platform for rapid access to gram-scale quantities of novel drug-like molecules. Metab. Eng. **42,** 185-193.

Reuben, S., Cseke, L.J., Bhinu, V.S., Narasimhan, K., Jeyakumar, M., and Swarup, S. (2006). Molecular biology of plant natural products. In Natural products from plants, L.J. Cseke, A. Kirakosyan, P.B. Kaufman, S.L. Warber, J.A. Duke, and H.L. Brielmann, eds (Boca Raton: CRC Press/Taylor & Francis), pp. 611-202.

Ross, J., Li, Y., Lim, E., and Bowles, D.J. (2001). Higher plant glycosyltransferases. Genome Biol **2,** REVIEWS3004.

Sainsbury, F., Thuenemann, E.C., and Lomonossoff, G.P. (2009). pEAQ: versatile expression vectors for easy and quick transient expression of heterologous proteins in plants. Plant Biotechnol. J. **7,** 682-693.

Sali, A., and Blundell, T.L. (1993). Comparative protein modelling by satisfaction of spatial restraints. J. Mol. Biol. **234,** 779-815.

Sawai, S., and Saito, K. (2011). Triterpenoid biosynthesis and engineering in plants. Front Plant Sci **2,** 25.

Sayama, T., Ono, E., Takagi, K., Takada, Y., Horikawa, M., Nakamoto, Y., Hirose, A., Sasama, H., Ohashi, M., Hasegawa, H., Terakawa, T.,

Kikuchi, A., Kato, S., Tatsuzaki, N., Tsukamoto, C., and Ishimoto, M. (2012). The *Sg-1* glycosyltransferase locus regulates structural diversity of triterpenoid saponins of soybean. Plant Cell **24,** 2123-2138.

Shao, H., He, X., Achnine, L., Blount, J.W., Dixon, R.A., and Wang, X. (2005). Crystal structures of a multifunctional triterpene/flavonoid glycosyltransferase from *Medicago truncatula*. Plant Cell **17,** 3141-3154.

Shibuya, M., Nishimura, K., Yasuyama, N., and Ebizuka, Y. (2010). Identification and characterization of glycosyltransferases involved in the biosynthesis of soyasaponin I in *Glycine max*. FEBS Lett. **584,** 2258-2264.

Tohge, T., Nishiyama, Y., Hirai, M.Y., Yano, M., Nakajima, J., Awazuhara, M., Inoue, E., Takahashi, H., Goodenowe, D.B., Kitayama, M., Noji, M., Yamazaki, M., and Saito, K. (2005). Functional genomics by integrated analysis of metabolome and transcriptome of Arabidopsis plants over-expressing an MYB transcription factor. Plant J. **42,** 218-235.

Tyanova, S., Temu, T., and Cox, J. (2016). The MaxQuant computational platform for mass spectrometry-based shotgun proteomics. Nat Protoc **11,** 2301-2319.

Van Der Spoel, D., Lindahl, E., Hess, B., Groenhof, G., Mark, A.E., and Berendsen, H.J. (2005). GROMACS: fast, flexible, and free. J Comput Chem **26,** 1701-1718.

Vetter, J. (2000). Plant cyanogenic glycosides. Toxicon **38,** 11-36.

Vincken, J.P., Heng, L., de Groot, A., and Gruppen, H. (2007). Saponins, classification and occurrence in the plant kingdom. Phytochemistry **68,** 275-297.

Vogt, T., and Jones, P. (2000). Glycosyltransferases in plant natural product synthesis: characterization of a supergene family. Trends Plant Sci. **5,** 380-386.

Wang, P., Wei, Y., Fan, Y., Liu, Q., Wei, W., Yang, C., Zhang, L., Zhao, G., Yue, J., Yan, X., and Zhou, Z. (2015). Production of bioactive ginsenosides Rh2 and Rg3 by metabolically engineered yeasts. Metab. Eng. **29,** 97-105.

Wei, W., Wang, P., Wei, Y., Liu, Q., Yang, C., Zhao, G., Yue, J., Yan, X., and Zhou, Z. (2015). Characterization of *Panax ginseng* UDP-glycosyltransferases catalyzing protopanaxatriol and biosyntheses of bioactive ginsenosides F1 and Rh1 in metabolically engineered yeasts. Mol Plant **8,** 1412-1424.

Wetterhorn, K.M., Newmister, S.A., Caniza, R.K., Busman, M., McCormick, S.P., Berthiller, F., Adam, G., and Rayment, I. (2016). Crystal Structure of Os79 (Os04g0206600) from *Oryza sativa*: A UDP-glucosyltransferase Involved in the Detoxification of Deoxynivalenol. Biochemistry **55,** 6175-6186.

Xu, G.J., Cai, W., Gao, W., and Liu, C.S. (2016). A novel glucuronosyltransferase has an unprecedented ability to catalyse continuous two-step glucuronosylation of glycyrrhetinic acid to yield glycyrrhizin. New Phytol. **212,** 123-135.

Yang, J., Yan, R., Roy, A., Xu, D., Poisson, J., and Zhang, Y. (2015). The I-TASSER Suite: protein structure and function prediction. Nat. Methods **12,** 7-8.

Yonekura-Sakakibara, K., Tohge, T., Matsuda, F., Nakabayashi, R., Takayama, H., Niida, R., Watanabe-Takahashi, A., Inoue, E., and Saito, K. (2008). Comprehensive flavonol profiling and transcriptome coexpression analysis leading to decoding gene-metabolite correlations in Arabidopsis. Plant Cell **20,** 2160-2176.

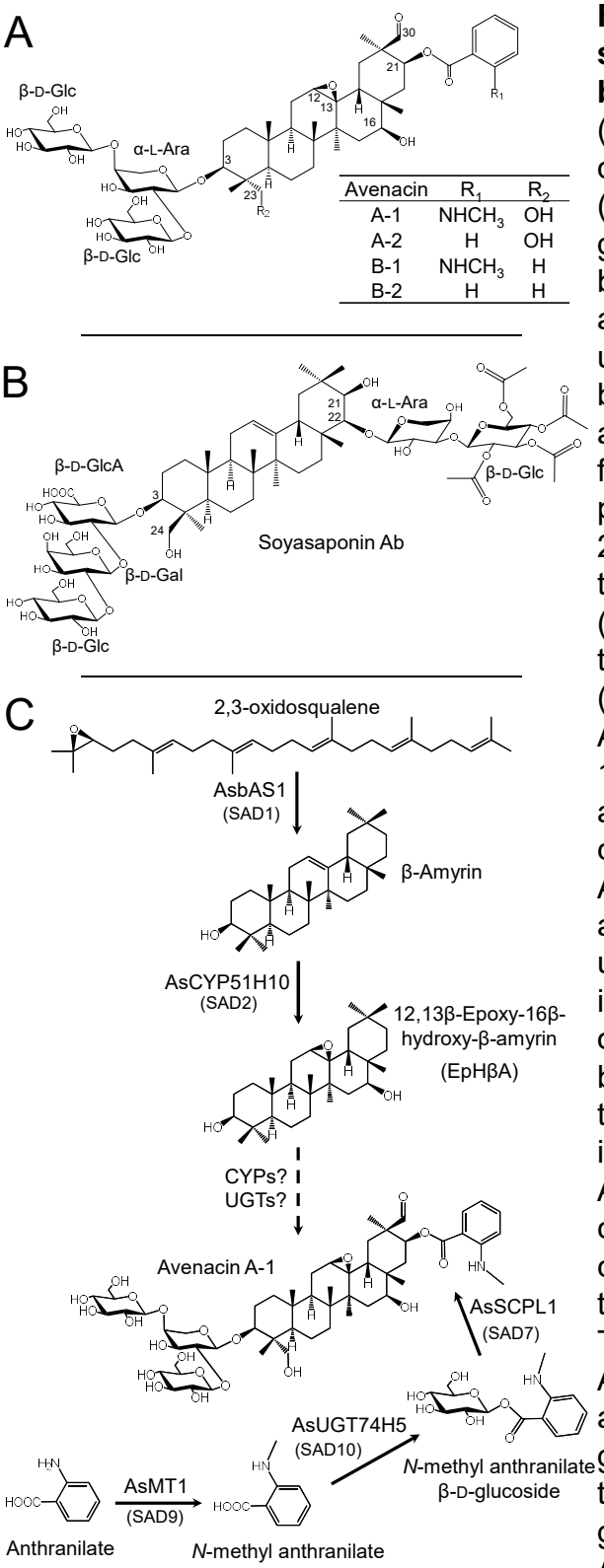

Figure 1. Triterpene glycoside structures and avenacin biosynthesis.
(A) Avenacins: antifungal defense compounds from oat. (B) Soyasaponin Ab, a triterpene glycoside associated with bitterness and anti-feedant activity in soybean. (C) Current understanding of the avenacin biosynthetic pathway. The major avenacin, A-1, is synthesised from the linear isoprenoid precursor 2,3-oxidosqualene. 2,3-Oxidosqualene is cyclized by the triterpene synthase AsbAS1 (SAD1) to the pentacyclic triterpene scaffold β-amyrin (Haralampidis et al., 2001). β-Amyrin is then oxidized to 12,13β-epoxy-16β-hydroxy-β-amyrin (EpHβA) by the cytochrome P450 enzyme AsCYP51H10 (SAD2) (Geisler et al., 2013). Subsequent, as-yet uncharacterized modifications involve a series of further oxygenations and addition of a branched trisaccharide moiety at the C-3 position, initiated by introduction of an L-arabinose. Acylation at the C-21 position is carried out by the serine carboxypeptidase-like acyl transferase AsSCPL1 (SAD7). The acyl donor used by AsSCPL1 is *N*-methyl anthranilate glucoside, which is generated by the methyl transferase AsMT1 and the glucosyl transferase AsUGT74H5 (SAD10) (Mugford et al., 2009; Owatworakit et al., 2012; Mugford et al., 2013).

Fig. 2

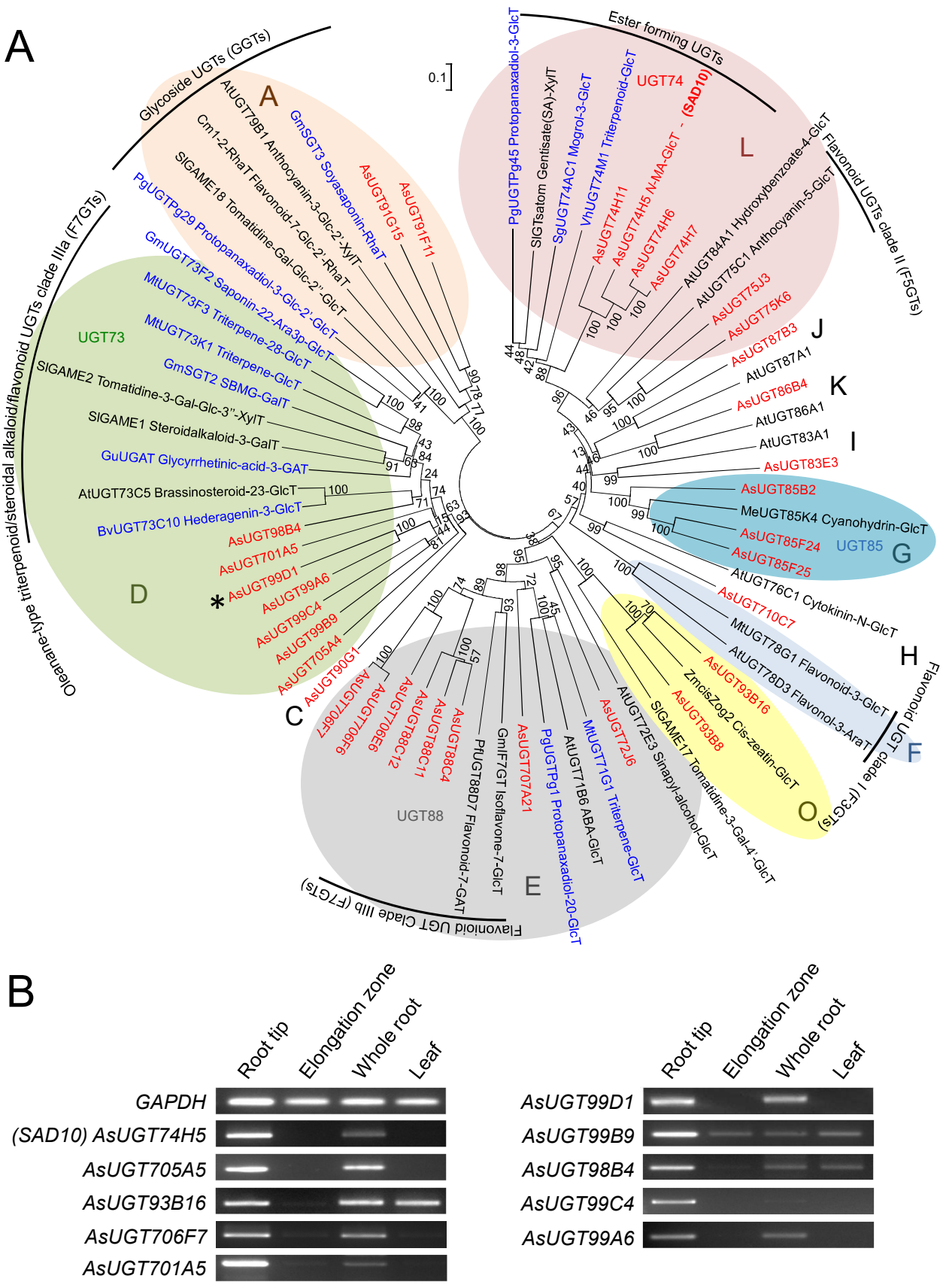
A
Glycoside UGTs (GGTs)
Ester forming UGTs
Flavonoid UGTs clade II (F5GTs)
Oleanane-type triterpenoid/steroidal alkaloid/flavonoid UGTs clade IIIa (F7GTs)
Flavonoid UGT clade IIIb (F7GTs)
Flavonoid UGT clade I (F3GTs)
0.1
A
L
J
K
I
G
H
F
O
E
C
D
UGT74
UGT85
UGT88
UGT73
AtUGT79B1 Anthocyanin-3-Glc-2'-XylT
Cm1-2-RhaT Flavonoid-7-Glc-2'-RhaT
SlGAME18 Tomatidine-Gal-Glc-2''-GlcT
PgUGTP929 Protopanaxadiol-3-Glc-2'-GlcT
GmUGT73F2 Saponin-22-Ara3p-GlcT
MtUGT73F3 Triterpene-28-GlcT
MtUGT73K1 Triterpene-GlcT
GmSGT2 SBMG-GalT
SlGAME2 Tomatidine-3-Gal-Glc-3''-XylT
SlGAME1 Steroidalkaloid-3-GalT
GuUGAT Glycyrrhetinic-acid-3-GAT
AtUGT73C5 Brassinosteroid-23-GlcT
BvUGT73C10 Hederagenin-3-GlcT
AsUGT98B4
AsUGT701A5
AsUGT99D1
AsUGT99A6
AsUGT99C4
AsUGT99B9
AsUGT705A4
AsUGT90G1
GmSGT3 Soyasaponin-RhaT
AsUGT91G15
AsUGT91F11
PgUGTPg45 Protopanaxadiol-3-GlcT
SlGTsatom Gentisate(SA)-XylT
SgUGT74AC1 Mogrol-3-GlcT
VhUGT74M1 Triterpenoid-GlcT
AsUGT74H11
AsUGT74H5 N-MA-GlcT - (SAD10)
AsUGT74H6
AsUGT74H7
AtUGT84A1 Hydroxybenzoate-4-GlcT
AtUGT75C1 Anthocyanin-5-GlcT
AsUGT75J3
AsUGT75K6
AsUGT87B3
AtUGT87A1
AsUGT86B4
AtUGT86A1
AtUGT83A1
AsUGT83E3
AsUGT85B2
MeUGT85K4 Cyanohydrin-GlcT
AsUGT85F24
AsUGT85F25
AtUGT76C1 Cytokinin-N-GlcT
AsUGT710C7
MtUGT78G1 Flavonoid-3-GlcT
AtUGT78D3 Flavonol-3-AraT
AsUGT93B16
AsUGT93B8
ZmcisZog2 Cis-zeatin-GlcT
SlGAME17 Tomatidine-3-Gal-4-GlcT
AtUGT72E3 Sinapyl-alcohol-GlcT
AsUGT72J6
MtUGT71G1 Triterpene-GlcT
AtUGT71B6 ABA-GlcT
PgUGTPg1 Protopanaxadiol-20-GlcT
AsUGT707A21
GmIF7GT Isoflavone-7-GlcT
PfUGT88D7 Flavonoid-7-GAT
AsUGT88C4
AsUGT88C11
AsUGT88C12
AsUGT706E6
AsUGT706F6
AsUGT706F7
B
Root tip
Elongation zone
Whole root
Leaf
GAPDH
(SAD10) AsUGT74H5
AsUGT705A5
AsUGT93B16
AsUGT706F7
AsUGT701A5
AsUGT99D1
AsUGT99B9
AsUGT98B4
AsUGT99C4
AsUGT99A6

Figure 2. Mining for candidate avenacin glycosyltransferase genes.
(A) Phylogenetic tree of UGTs expressed in *A. strigosa* root tips (red) (listed in Supplemental Table 3). Characterized triterpenoid glycosyltransferases from other plant species (blue) and other biochemically characterized plant UGTs (black) are also included (listed in Supplemental Table 4). The UGT groups are as defined by Ross et al. (2001). Some of the most common groups of enzyme activities are indicated. The tree was constructed using the Neighbour Joining method with 1000 bootstrap replicates (% support for branch points shown). The scale bar indicates 0.1 substitutions per site at the amino acid level. The alignment file is available as Supplemental Data set 1. (B) Expression profiles of selected oat UGT genes (RT-PCR). Tissues were collected from 3-day-old *A. strigosa* seedlings. The characterized avenacin biosynthetic gene *AsUGT74H5* (*Sad10*) and the glyceraldehyde 3-phosphate dehydrogenase (*GAPDH*) housekeeping gene are included as controls.

Fig. 3

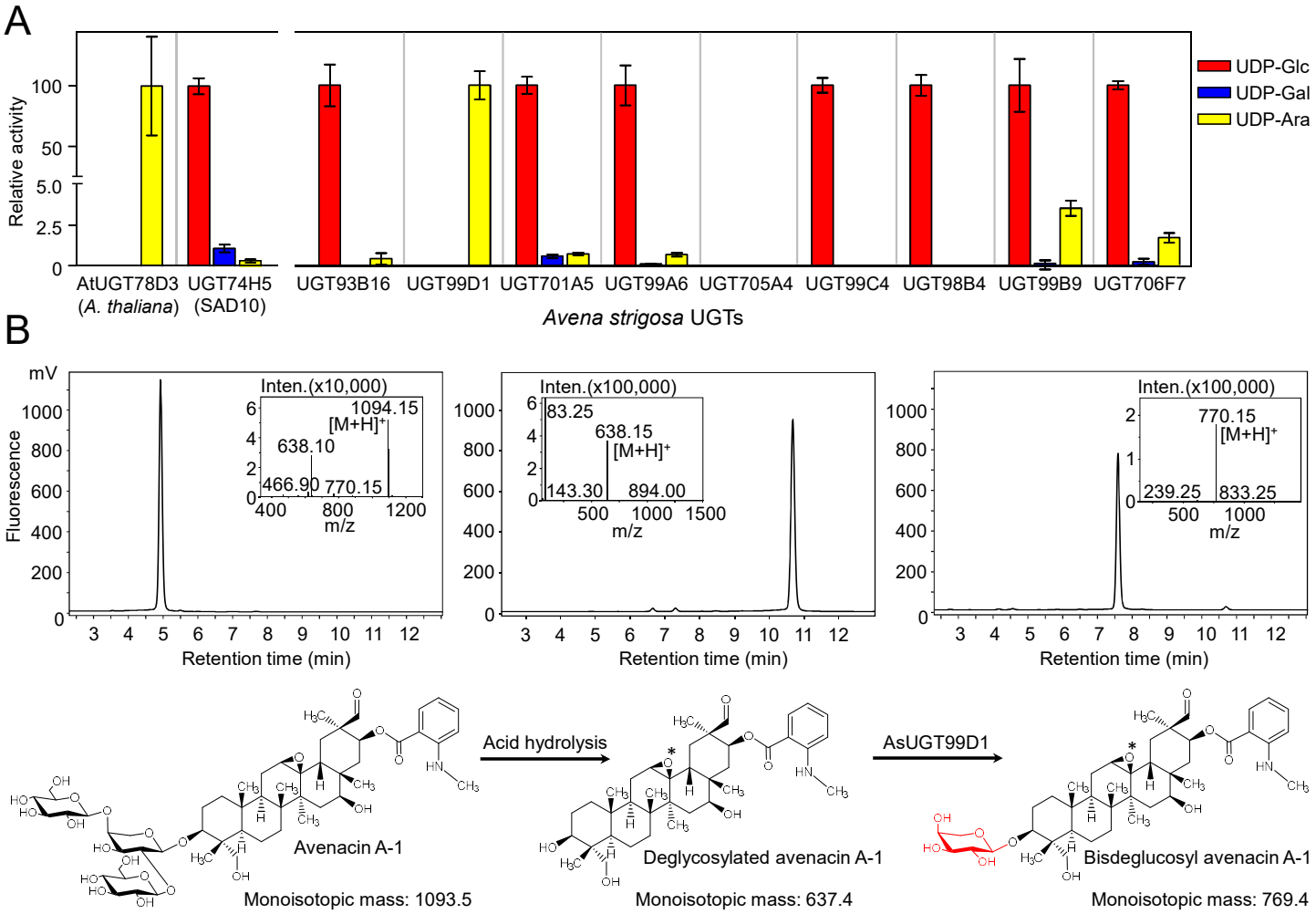

Figure 3. Biochemical characterization of candidate oat UGTs.
(A) Evaluation of sugar donor specificity of recombinant oat UGTs using the universal acceptor 2,4,5-trichlorophenol (TCP). Relative activities with different sugar nucleotide donors are shown. Conversion of TCP to TCP glycoside was monitored by spectrophotometry at 405 nm. The previously characterized oat *N*-methyl anthranilate glucosyltransferase AsUGT74H5 (SAD10) and *A. thaliana* flavonoid arabinosyltransferase UGT78D3 were included as controls. Values are means of three biological replicates; error bars represent standard deviations. (B) LC-MS profiles for avenacin A-1 (left), deglycosylated avenacin A-1 (middle), and the product generated by incubation of deglycosylated avenacin A-1 with AsUGT99D1 (right) (detection by fluorescence; excitation and emission wavelengths 353 and 441 nm, respectively). The hydrolyzed avenacin product is shown with an intact 12,13-epoxide (*), but this epoxide may have rearranged to a ketone under the acidic hydrolysis conditions resulting in deglycosylated 12-oxo-avenacin A-1, as observed previously (Geisler et al., 2013).

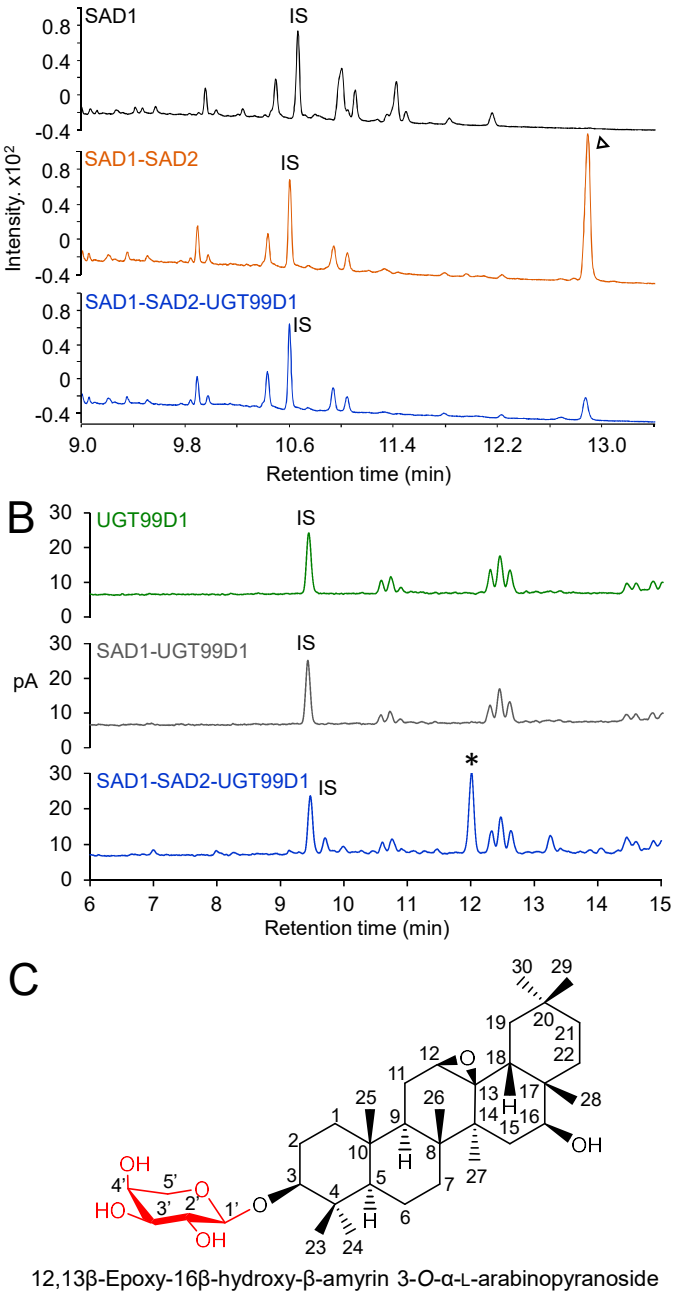

12,13β-Epoxy-16β-hydroxy-β-amyrin 3-*O*-α-L-arabinopyranoside

Figure 4. Transient expression of AsAAT1 in *Nicotiana benthamiana.*
(A) GC-MS analysis of extracts from agro-infiltrated *N. benthamiana* leaves. Comparison of the metabolite profiles of leaves expressing SAD1 and SAD2 (red) or SAD1, SAD2 and UGT99D1 (blue). EpHβA , identified previously as the co-expression product of SAD1 and SAD2 is indicated by an arrow (Geisler et al., 2013). The upper chromatogram consists of a control from leaves expressing GFP only (black). (B) HPLC with charged aerosol detection (CAD) chromatograms of extracts from *N. benthamiana* leaves expressing UGT99D1 alone (green), SAD1 and UGT99D1 (grey) and SAD1, SAD2 and UGT99D1 together (blue). The new compound that accumulated in the latter (tR 12.0 min) is indicated by an asterisk. This compound was not detected when UGT99D1 was expressed on its own or with SAD1. The internal standard (IS) was digitoxin (1 mg/g of dwt). (C) Structure of the UGT99D1 product (see Supplemental Figure 4 for NMR assignment).

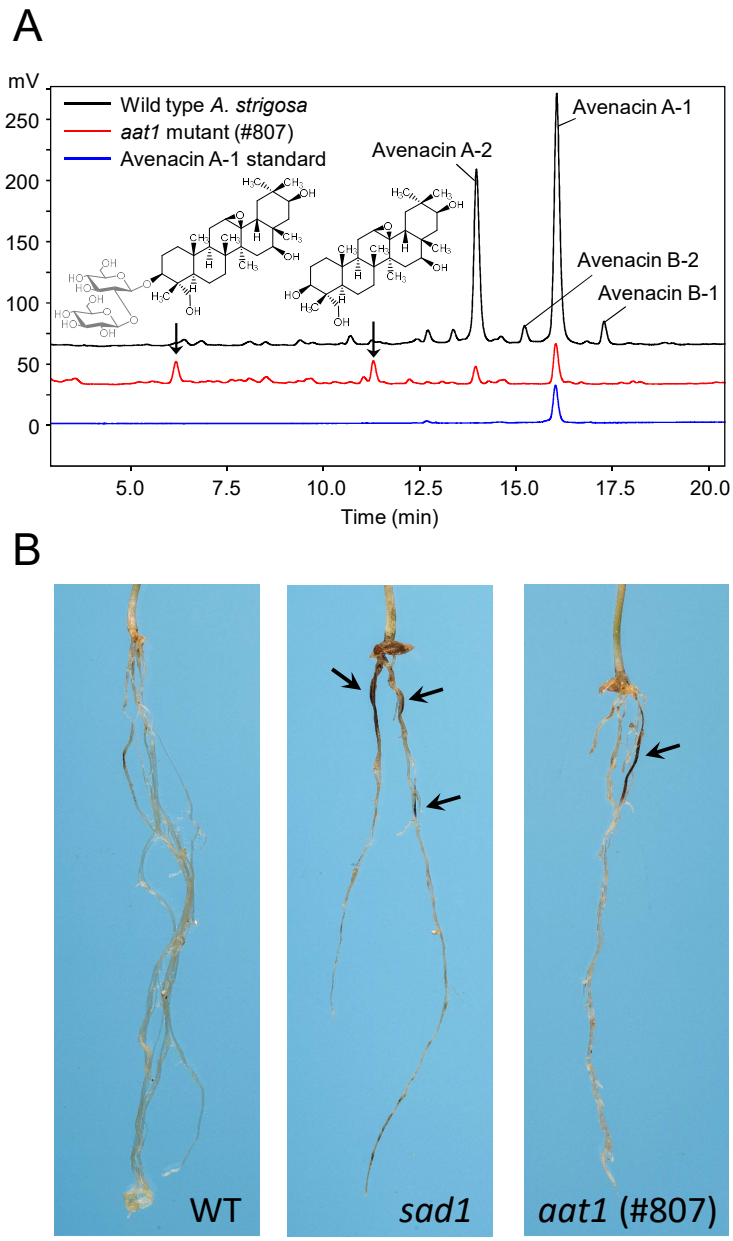

Figure 5. Biochemical analysis of *aat1* mutant and susceptibility to take-all disease. (A) HPLC-CAD analysis of methanolic root extracts from seedlings of the *A. strigosa* wild-type accession and avenacin-deficient mutant line #807 (*aat1*). New metabolites detected in the mutant are arrowed and inferred structures are shown based on the corresponding ion chromatograms (Supplemental Figure 5D). (B) *aat1* (#807) has enhanced disease susceptibility. Images of representative seedlings of wild-type *A. strigosa* (WT), the *sad1* mutant #610 (Haralampidis et al., 2001), and the *aat1* mutant (this study) are shown. Seedlings were inoculated with the take-all fungus (*G. graminis* var. *tritici*). The dark lesions on the roots are symptoms of infection and are indicated by arrows.

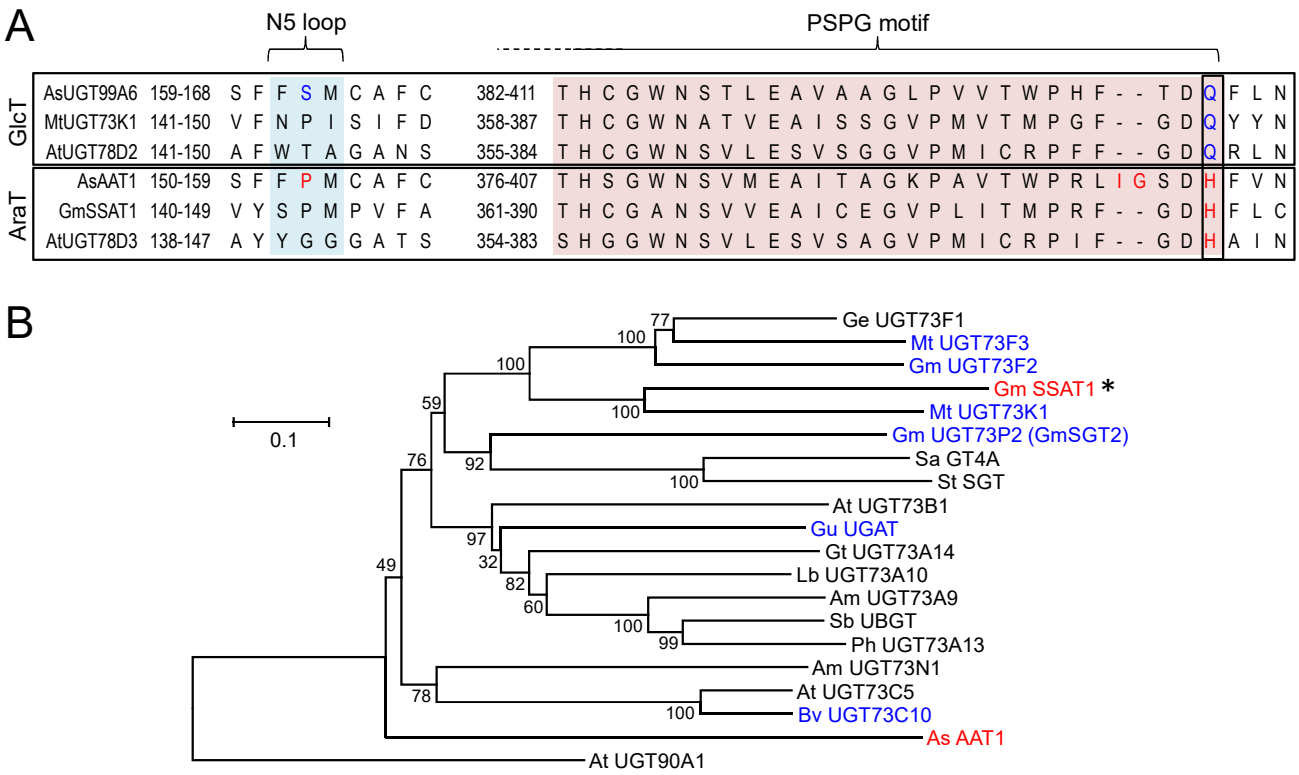

Figure 6. An arabinosyltransferase from soybean.
(A) Alignment of the amino acid sequences of the oat, soybean and *A. thaliana* arabinosyltransferases with the closest characterized glucosyltransferases in the region of the PSPG motif and the N5 loop. The histidine residue that is conserved in the arabinosyltransferases is shown in red. P154 and the two additional amino acids IG of AsAAT1 are also highlighted. (B) Phylogenetic analysis of glycosyltransferases from group D belonging to the UGT73 family. GmSSAT1 and AsAAT1 are indicated in red, and other characterized triterpenoid glycosyltransferases in blue (see Supplemental Table 4 for further details). The tree was constructed using the Neighbour Joining method with 1000 bootstrap replicates (percentage support shown at branch points), and rooted with UGT90A1, an *A. thaliana* UGT from group C. The scale bar indicates 0.1 substitutions per site at the amino acid level. The alignment file is available as Supplemental Data set 3.

Fig. 7

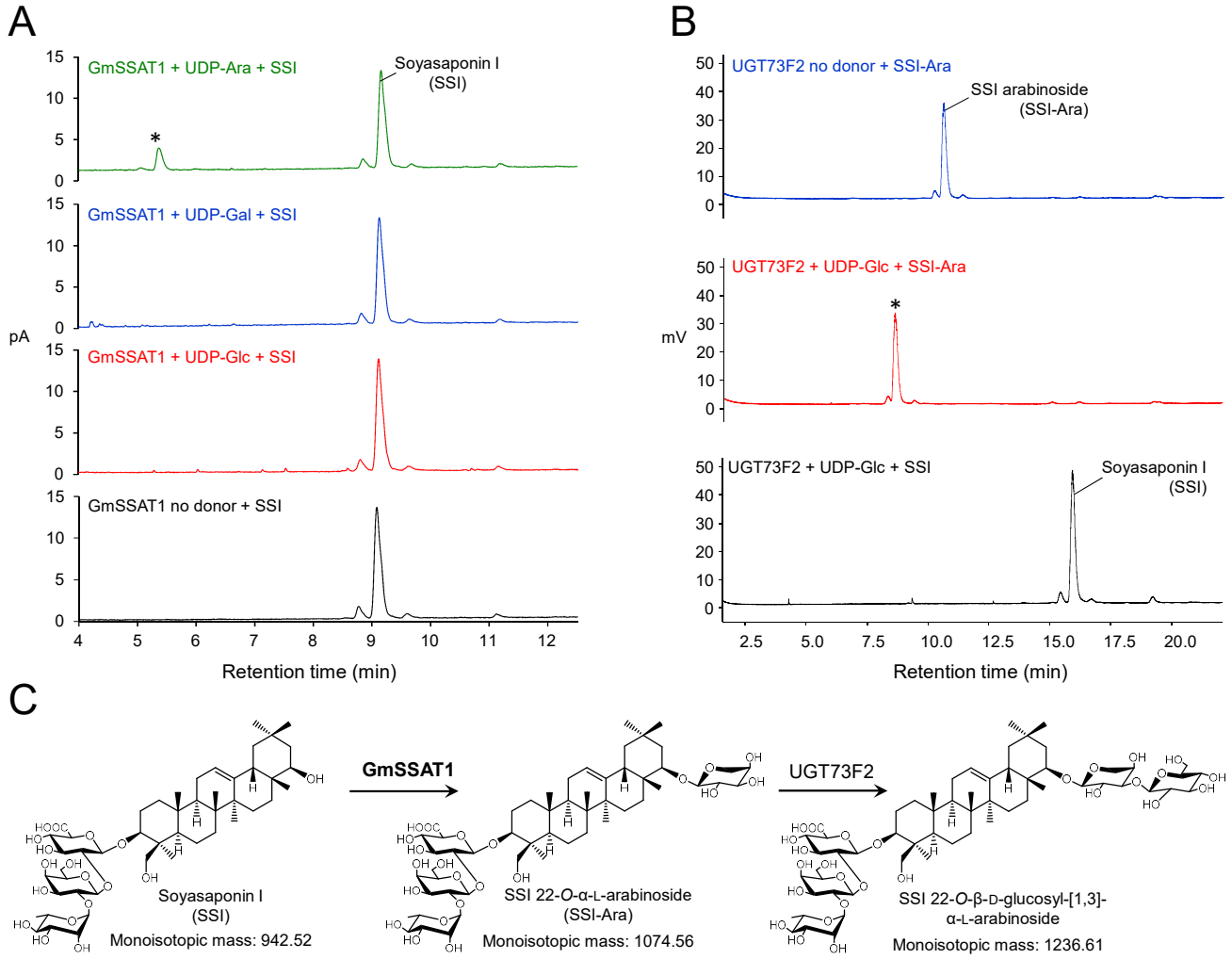

Figure 7. Biochemical characterization of GmSSAT1.
(A) HPLC-CAD chromatogram of *in vitro* assays performed with recombinant GmSSAT1 and different UDP-sugars. GmSSAT1 was incubated for 40 min at 25°C with 100 µM soyasaponin I (SSI) and 300 µM UDP-sugars. A major product is detected only in the presence of UDP-Ara (*) (see Supplemental Figure 7A for MS analysis). (B) HPLC-CAD analysis of reactions in which the previously characterized soyasaponin glucosyltransferase UGT73F2 (Sayama et al., 2012) was assayed for activity towards the GmSSAT1 product. Recombinant UGT73F2 was incubated overnight with 400 µM UDP-Glc and approximately 100 µM of the GmSSAT1 product SSI-22-O-α-L-arabinoside (SSI-Ara). SSI-Ara (t_R: 10.6 min) was completely converted to a new product with a t_R of 8.6 min (asterisked). MS analysis of this product is shown in Supplemental Figure 7B. No product was detected in the absence of UDP-Glc or if the acceptor was replaced by SSI. (C) Schematic showing successive glycosylation of soyasaponin I by GmSSAT1 and UGT73F2.

Fig. 8

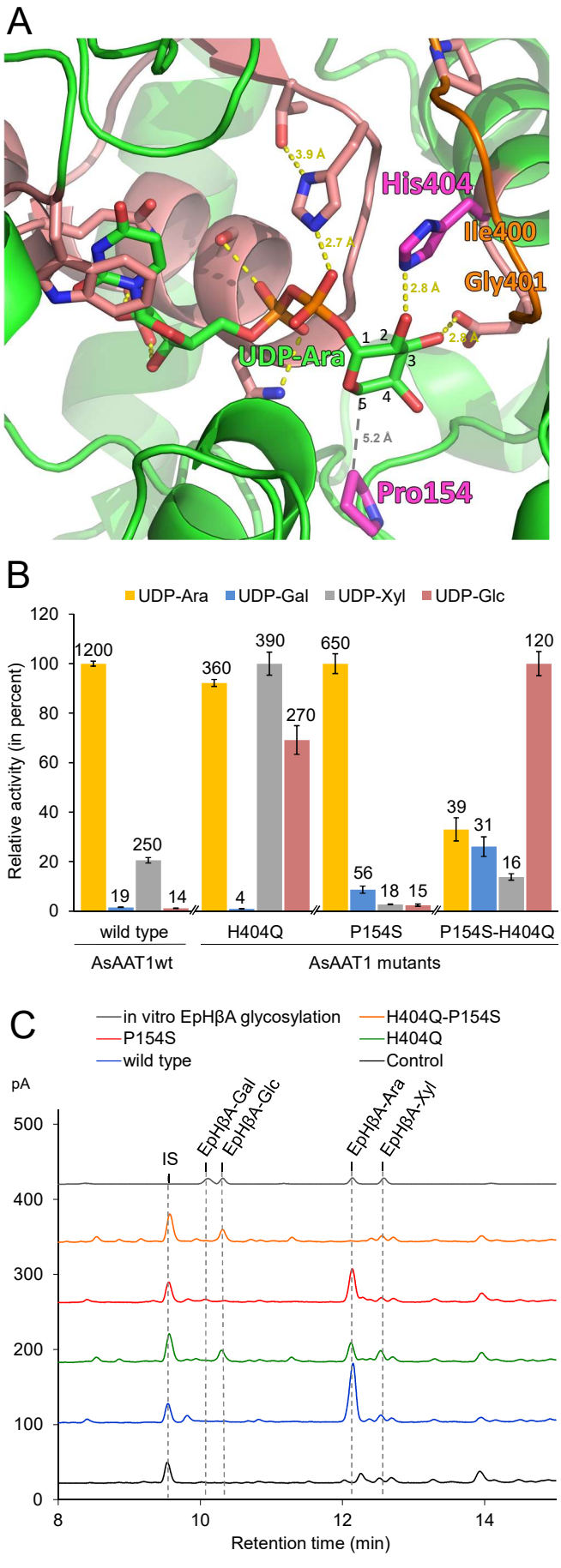
A
3.9 Å
2.7 Å
2.8 Å
2.6 Å
His404
Ile400
Gly401
UDP-Ara
1
2
3
4
5
5.2 Å
Pro154
B
UDP-Ara
UDP-Gal
UDP-Xyl
UDP-Glc
Relative activity (in percent)
120
100
80
60
40
20
0
1200
19
250
14
360
4
390
270
650
56
18
15
39
31
16
120
wild type
H404Q
P154S
P154S-H404Q
AsAAT1wt
AsAAT1 mutants
C
in vitro EpHβA glycosylation
P154S
wild type
H404Q-P154S
H404Q
Control
pA
500
400
300
200
100
0
IS
EpHβA-Gal
EpHβA-Glc
EpHβA-Ara
EpHβA-Xyl
8
10
12
14
Retention time (min)

Figure 8. Determinants of sugar donor sugar specificity of AsAAT1.
(A) Model of AsAAT1 with bound UDP-Ara (carbons of the arabinose numbered). The protein is represented in green ribbons with the PSPG motif in salmon, including the side chains of highly conserved residues. The His404 and Pro154 residues are shown in magenta. Potential hydrogen bonds are shown with yellow dots, and the distance between P154 and C-5 of UDP-Ara with grey dots The homology model was generated using I-TASSER software (Yang et al., 2015), based on the crystal structure of *Medicago truncatula* UGT71G1 complexed with UDP-Glc (PDB: 2ACW). The loop shown in orange was reconstructed using MODELLER (Sali and Blundell, 1993). UDP-Ara was inserted into the active site and the complex was relaxed for energy minimization using GROMACS. (B) Comparison of the glycosylation activity of the AsAAT1 wild-type and mutant enzymes when supplied with each of the four sugar donors (UDP-Ara, UDP-Gal, UDP-Xyl or UDP-Glc). Initial velocities were measured using 30 µM deglycosylated avenacin A-1 as acceptor and 5 µM UDP-sugar donor using five timepoints. The heights of the bars are drawn relative to the highest activity observed for each recombinant enzyme (mean ± SD, n = 3). Activities reported above each bar are in nM.min-1. (C) HPLC-CAD analysis of extracts from *N. benthamiana* leaves expressing SAD1 and SAD2 together with GFP (black), wild-type AsAAT1 enzyme (blue), AsAAT1-H404Q (green), AsAAT1-P154S (red) and AsAAT1-H404Q-P154S (orange). The top trace (in grey) shows the products of in vitro reaction of 12,13β-epoxy-16β-hydroxy-β-amyrin (EpHβA) with the four sugar donors (reactions carried out separately and then pooled) for reference. LC-MS analysis was used to confirm the identities of the new products (Supplemental Figure 8C). The internal standard (IS) is digitoxin (1 mg/g dwt).

Parsed Citations

Achnine, L., Huhman, D.V., Farag, M.A., Sumner, L.W., Blount, J.W., and Dixon, R.A. (2005). Genomics-based selection and functional characterization of triterpene glycosyltransferases from the model legume Medicago truncatula. Plant J. 41, 875-887.
Pubmed: Author and Title
Google Scholar: Author Only Title Only Author and Title

Armah, C.N., Mackie, A.R., Roy, C., Price, K., Osbourn, A.E., Bowyer, P., and Ladha, S. (1999). The membrane-permeabilizing effect of avenacin A-1 involves the reorganization of bilayer cholesterol. Biophys. J. 76, 281-290.
Pubmed: Author and Title
Google Scholar: Author Only Title Only Author and Title

Augustin, J.M., Kuzina, V., Andersen, S.B., and Bak, S. (2011). Molecular activities, biosynthesis and evolution of triterpenoid saponins. Phytochemistry 72, 435-457.
Pubmed: Author and Title
Google Scholar: Author Only Title Only Author and Title

Augustin, J.M., Drok, S., Shinoda, T., Sanmiya, K., Nielsen, J.K., Khakimov, B., Olsen, C.E., Hansen, E.H., Kuzina, V., Ekstrom, C.T., Hauser, T., and Bak, S. (2012). UDP-glycosyltransferases from the UGT73C subfamily in Barbarea vulgaris catalyze sapogenin 3-O-glucosylation in saponin-mediated insect resistance. Plant Physiol. 160, 1881-1895.
Pubmed: Author and Title
Google Scholar: Author Only Title Only Author and Title

Benkert, P., Tosatto, S.C., and Schomburg, D. (2008). QMEAN: A comprehensive scoring function for model quality assessment. Proteins 71, 261-277.
Pubmed: Author and Title
Google Scholar: Author Only Title Only Author and Title

Bernard, F.X., Sable, S., Cameron, B., Provost, J., Desnottes, J.F., Crouzet, J., and Blanche, F. (1997). Glycosylated flavones as selective inhibitors of topoisomerase IV. Antimicrob. Agents Chemother. 41, 992-998.
Pubmed: Author and Title
Google Scholar: Author Only Title Only Author and Title

Bowles, D., Lim, E.K., Poppenberger, B., and Vaistij, F.E. (2006). Glycosyltransferases of lipophilic small molecules. Annu. Rev. Plant Biol. 57, 567-597.
Pubmed: Author and Title
Google Scholar: Author Only Title Only Author and Title

Bradford, M.M. (1976). A rapid and sensitive method for the quantitation of microgram quantities of protein utilizing the principle of protein-dye binding. Anal. Biochem. 72, 248-254.
Pubmed: Author and Title
Google Scholar: Author Only Title Only Author and Title

Caputi, L., Lim, E.K., and Bowles, D.J. (2008). Discovery of new biocatalysts for the glycosylation of terpenoid scaffolds. Chemistry 14, 6656-6662.
Pubmed: Author and Title
Google Scholar: Author Only Title Only Author and Title

Caputi, L., Malnoy, M., Goremykin, V., Nikiforova, S., and Martens, S. (2011). A genome-wide phylogenetic reconstruction of family 1 UDP-glycosyltransferases revealed the expansion of the family during the adaptation of plants to life on land. Plant J. 69, 1030-1042.
Pubmed: Author and Title
Google Scholar: Author Only Title Only Author and Title

Chen, V.B., Arendall, W.B., 3rd, Headd, J.J., Keedy, D.A., Immormino, R.M., Kapral, G.J., Murray, L.W., Richardson, J.S., and Richardson, D.C. (2010). MolProbity: all-atom structure validation for macromolecular crystallography. Acta Crystallogr D Biol Crystallogr 66, 12-21.
Pubmed: Author and Title
Google Scholar: Author Only Title Only Author and Title

Dai, L., Liu, C., Zhu, Y., Zhang, J., Men, Y., Zeng, Y., and Sun, Y. (2015). Functional characterization of cucurbitadienol synthase and triterpene glycosyltransferase involved in biosynthesis of mogrosides from Siraitia grosvenorii. Plant Cell Physiol. 56, 1172-1182.
Pubmed: Author and Title
Google Scholar: Author Only Title Only Author and Title

Francis, G., Kerem, Z., Makkar, H.P., and Becker, K. (2002). The biological action of saponins in animal systems: a review. Br J Nutr 88, 587-605.
Pubmed: Author and Title
Google Scholar: Author Only Title Only Author and Title

Gachon, C.M., Langlois-Meurinne, M., and Saindrenan, P. (2005). Plant secondary metabolism glycosyltransferases: the emerging functional analysis. Trends Plant Sci. 10, 542-549.
Pubmed: Author and Title
Google Scholar: Author Only Title Only Author and Title

Geisler, K., Hughes, R.K., Sainsbury, F., Lomonossoff, G.P., Rejzek, M., Fairhurst, S., Olsen, C.E., Motawia, M.S., Melton, R.E.,

Hemmings, A.M., Bak, S., and Osbourn, A. (2013). Biochemical analysis of a multifunctional cytochrome P450 (CYP51) enzyme required for synthesis of antimicrobial triterpenes in plants. Proc Natl Acad Sci U S A 110, 3360-3367.
Pubmed: Author and Title
Google Scholar: Author Only Title Only Author and Title

Grille, S., Zaslawski, A., Thiele, S., Plat, J., and Warnecke, D. (2010). The functions of steryl glycosides come to those who wait: Recent advances in plants, fungi, bacteria and animals. Prog Lipid Res 49, 262-288.
Pubmed: Author and Title
Google Scholar: Author Only Title Only Author and Title

Han, S.H., Kim, B.G., Yoon, J.A., Chong, Y., and Ahn, J.H. (2014). Synthesis of flavonoid O-pentosides by Escherichia coli through engineering of nucleotide sugar pathways and glycosyltransferase. Appl. Environ. Microbiol. 80, 2754-2762.
Pubmed: Author and Title
Google Scholar: Author Only Title Only Author and Title

Haralampidis, K., Bryan, G., Qi, X., Papadopoulou, K., Bakht, S., Melton, R., and Osbourn, A. (2001). A new class of oxidosqualene cyclases directs synthesis of antimicrobial phytoprotectants in monocots. Proc Natl Acad Sci U S A 98, 13431-13436.
Pubmed: Author and Title
Google Scholar: Author Only Title Only Author and Title

Hartley, J.L., Temple, G.F., and Brasch, M.A. (2000). DNA cloning using in vitro site-specific recombination. Genome Res. 10, 1788-1795.
Pubmed: Author and Title
Google Scholar: Author Only Title Only Author and Title

He, X.Z., Wang, X., and Dixon, R.A. (2006). Mutational analysis of the Medicago glycosyltransferase UGT71G1 reveals residues that control regioselectivity for (iso)flavonoid glycosylation. J. Biol. Chem. 281, 34441-34447.
Pubmed: Author and Title
Google Scholar: Author Only Title Only Author and Title

Hughes, J., and Hughes, M.A. (1994). Multiple secondary plant product UDP-glucose glucosyltransferase genes expressed in cassava (Manihot esculenta Crantz) cotyledons. DNA Seq 5, 41-49.
Pubmed: Author and Title
Google Scholar: Author Only Title Only Author and Title

Kemen, A.C., Honkanen, S., Melton, R.E., Findlay, K.C., Mugford, S.T., Hayashi, K., Haralampidis, K., Rosser, S.J., and Osbourn, A. (2014). Investigation of triterpene synthesis and regulation in oats reveals a role for beta-amyrin in determining root epidermal cell patterning. Proc Natl Acad Sci U S A 111, 8679-8684.
Pubmed: Author and Title
Google Scholar: Author Only Title Only Author and Title

Kubo, A., Arai, Y., Nagashima, S., and Yoshikawa, T. (2004). Alteration of sugar donor specificities of plant glycosyltransferases by a single point mutation. Arch Biochem Biophys 429, 198-203.
Pubmed: Author and Title
Google Scholar: Author Only Title Only Author and Title

Li, Y., Baldauf, S., Lim, E.K., and Bowles, D.J. (2001). Phylogenetic analysis of the UDP-glycosyltransferase multigene family of Arabidopsis thaliana. J. Biol. Chem. 276, 4338-4343.
Pubmed: Author and Title
Google Scholar: Author Only Title Only Author and Title

Liu, Z., Liu, Y., Pu, Z., Wang, J., Zheng, Y., Li, Y., and Wei, Y. (2013). Regulation, evolution, and functionality of flavonoids in cereal crops. Biotechnol. Lett. 35, 1765-1780.
Pubmed: Author and Title
Google Scholar: Author Only Title Only Author and Title

Mackenzie, P.I., Owens, I.S., Burchell, B., Bock, K.W., Bairoch, A., Belanger, A., Fournel-Gigleux, S., Green, M., Hum, D.W., Iyanagi, T., Lancet, D., Louisot, P., Magdalou, J., Chowdhury, J.R., Ritter, J.K., Schachter, H., Tephly, T.R., Tipton, K.F., and Nebert, D.W. (1997). The UDP glycosyltransferase gene superfamily: recommended nomenclature update based on evolutionary divergence. Pharmacogenetics 7, 255-269.
Pubmed: Author and Title
Google Scholar: Author Only Title Only Author and Title

Meesapyodsuk, D., Balsevich, J., Reed, D.W., and Covello, P.S. (2007). Saponin biosynthesis in Saponaria vaccaria. cDNAs encoding beta-amyrin synthase and a triterpene carboxylic acid glucosyltransferase. Plant Physiol. 143, 959-969.
Pubmed: Author and Title
Google Scholar: Author Only Title Only Author and Title

Messner, B., Thulke, O., and Schaffner, A.R. (2003). Arabidopsis glucosyltransferases with activities toward both endogenous and xenobiotic substrates. Planta 217, 138-146.
Pubmed: Author and Title
Google Scholar: Author Only Title Only Author and Title

Mugford, S.T., Louveau, T., Melton, R., Qi, X., Bakht, S., Hill, L., Tsurushima, T., Honkanen, S., Rosser, S.J., Lomonossoff, G.P., and Osbourn, A. (2013). Modularity of plant metabolic gene clusters: A trio of linked genes that are collectively required for acylation of

triterpenes in oat. Plant Cell 25, 1078–1092.
Pubmed: Author and Title
Google Scholar: Author Only Title Only Author and Title

Mugford, S.T., Qi, X., Bakht, S., Hill, L., Wegel, E., Hughes, R.K., Papadopoulou, K., Melton, R., Philo, M., Sainsbury, F., Lomonossoff, G.P., Roy, A.D., Goss, R.J., and Osbourn, A. (2009). A serine carboxypeptidase-like acyltransferase is required for synthesis of antimicrobial compounds and disease resistance in oats. Plant Cell 21, 2473-2484.
Pubmed: Author and Title
Google Scholar: Author Only Title Only Author and Title

Mylona, P., Owatworakit, A., Papadopoulou, K., Jenner, H., Qin, B., Findlay, K., Hill, L., Qi, X., Bakht, S., Melton, R., and Osbourn, A. (2008). Sad3 and Sad4 are required for saponin biosynthesis and root development in oat. Plant Cell 20, 201-212.
Pubmed: Author and Title
Google Scholar: Author Only Title Only Author and Title

Naoumkina, M.A., Modolo, L.V., Huhman, D.V., Urbanczyk-Wochniak, E., Tang, Y., Sumner, L.W., and Dixon, R.A. (2010). Genomic and coexpression analyses predict multiple genes involved in triterpene saponin biosynthesis in Medicago truncatula. Plant Cell 22, 850-866.
Pubmed: Author and Title
Google Scholar: Author Only Title Only Author and Title

Noguchi, A., Horikawa, M., Fukui, Y., Fukuchi-Mizutani, M., Iuchi-Okada, A., Ishiguro, M., Kiso, Y., Nakayama, T., and Ono, E. (2009). Local differentiation of sugar donor specificity of flavonoid glycosyltransferase in Lamiales. Plant Cell 21, 1556-1572.
Pubmed: Author and Title
Google Scholar: Author Only Title Only Author and Title

O'Maille, P.E., Malone, A., Dellas, N., Andes Hess, B., Jr., Smentek, L., Sheehan, I., Greenhagen, B.T., Chappell, J., Manning, G., and Noel, J.P. (2008). Quantitative exploration of the catalytic landscape separating divergent plant sesquiterpene synthases. Nat. Chem. Biol. 4, 617-623.
Pubmed: Author and Title
Google Scholar: Author Only Title Only Author and Title

Oostenbrink, C., Villa, A., Mark, A.E., and van Gunsteren, W.F. (2004). A biomolecular force field based on the free enthalpy of hydration and solvation: the GROMOS force-field parameter sets 53A5 and 53A6. J Comput Chem 25, 1656-1676.
Pubmed: Author and Title
Google Scholar: Author Only Title Only Author and Title

Osbourn, A. (1996). Saponins and plant defence - a soap story. Trends Plant Sci. 1, 4-9.
Pubmed: Author and Title
Google Scholar: Author Only Title Only Author and Title

Osbourn, A., Bowyer, P., Lunness, P., Clarke, B., and Daniels, M. (1995). Fungal pathogens of oat roots and tomato leaves employ closely related enzymes to detoxify different host plant saponins. Mol Plant Microbe Interact 8, 971-978.
Pubmed: Author and Title
Google Scholar: Author Only Title Only Author and Title

Osmani, S.A., Bak, S., and Moller, B.L. (2009). Substrate specificity of plant UDP-dependent glycosyltransferases predicted from crystal structures and homology modeling. Phytochemistry 70, 325-347.
Pubmed: Author and Title
Google Scholar: Author Only Title Only Author and Title

Osmani, S.A., Bak, S., Imberty, A., Olsen, C.E., and Moller, B.L. (2008). Catalytic key amino acids and UDP-sugar donor specificity of a plant glucuronosyltransferase, UGT94B1: molecular modeling substantiated by site-specific mutagenesis and biochemical analyses. Plant Physiol. 148, 1295-1308.
Pubmed: Author and Title
Google Scholar: Author Only Title Only Author and Title

Owatworakit, A., Townsend, B., Louveau, T., Jenner, H., Rejzek, M., Hughes, R.K., Saalbach, G., Qi, X., Bakht, S., Deb Roy, A., Mugford, S.T., Goss, R.J., Field, R.A., and Osbourn, A. (2012). Glycosyltransferases from oat (Avena) implicated in the acylation of avenacins. J. Biol. Chem. 288, 3696-3704.
Pubmed: Author and Title
Google Scholar: Author Only Title Only Author and Title

Papadopoulou, K., Melton, R.E., Leggett, M., Daniels, M.J., and Osbourn, A.E. (1999). Compromised disease resistance in saponin-deficient plants. Proc Natl Acad Sci U S A 96, 12923-12928.
Pubmed: Author and Title
Google Scholar: Author Only Title Only Author and Title

Pettersen, E.F., Goddard, T.D., Huang, C.C., Couch, G.S., Greenblatt, D.M., Meng, E.C., and Ferrin, T.E. (2004). UCSF Chimera--a visualization system for exploratory research and analysis. J Comput Chem 25, 1605-1612.
Pubmed: Author and Title
Google Scholar: Author Only Title Only Author and Title

Piochon, M., Legault, J., Gauthier, C., and Pichette, A. (2009). Synthesis and cytotoxicity evaluation of natural alpha-bisabolol beta-D-

fucopyranoside and analogues. Phytochemistry 70, 228-236.
Pubmed: Author and Title
Google Scholar: Author Only Title Only Author and Title

Qi, X., Bakht, S., Leggett, M., Maxwell, C., Melton, R., and Osbourn, A. (2004). A gene cluster for secondary metabolism in oat: implications for the evolution of metabolic diversity in plants. Proc Natl Acad Sci U S A 101, 8233-8238.
Pubmed: Author and Title
Google Scholar: Author Only Title Only Author and Title

Qi, X., Bakht, S., Qin, B., Leggett, M., Hemmings, A., Mellon, F., Eagles, J., Werck-Reichhart, D., Schaller, H., Lesot, A., Melton, R., and Osbourn, A. (2006). A different function for a member of an ancient and highly conserved cytochrome P450 family: from essential sterols to plant defense. Proc Natl Acad Sci U S A 103, 18848-18853.
Pubmed: Author and Title
Google Scholar: Author Only Title Only Author and Title

Qin, B., Eagles, J., Mellon, F.A., Mylona, P., Pena-Rodriguez, L., and Osbourn, A.E. (2010). High throughput screening of mutants of oat that are defective in triterpene synthesis. Phytochemistry 71, 1245-1252.
Pubmed: Author and Title
Google Scholar: Author Only Title Only Author and Title

Reed, J., Stephenson, M.J., Miettinen, K., Brouwer, B., Leveau, A., Brett, P., Goss, R.J.M., Goossens, A., O'Connell, M.A., and Osbourn, A. (2017). A translational synthetic biology platform for rapid access to gram-scale quantities of novel drug-like molecules. Metab. Eng. 42, 185-193.
Pubmed: Author and Title
Google Scholar: Author Only Title Only Author and Title

Reuben, S., Cseke, L.J., Bhinu, V.S., Narasimhan, K., Jeyakumar, M., and Swarup, S. (2006). Molecular biology of plant natural products. In Natural products from plants, L.J. Cseke, A. Kirakosyan, P.B. Kaufman, S.L. Warber, J.A. Duke, and H.L. Brielmann, eds (Boca Raton: CRC Press/Taylor & Francis), pp. 611-202.
Pubmed: Author and Title
Google Scholar: Author Only Title Only Author and Title

Ross, J., Li, Y., Lim, E., and Bowles, D.J. (2001). Higher plant glycosyltransferases. Genome Biol 2, REVIEWS3004.
Pubmed: Author and Title
Google Scholar: Author Only Title Only Author and Title

Sainsbury, F., Thuenemann, E.C., and Lomonossoff, G.P. (2009). pEAQ: versatile expression vectors for easy and quick transient expression of heterologous proteins in plants. Plant Biotechnol. J. 7, 682-693.
Pubmed: Author and Title
Google Scholar: Author Only Title Only Author and Title

Sali, A., and Blundell, T.L. (1993). Comparative protein modelling by satisfaction of spatial restraints. J. Mol. Biol. 234, 779-815.
Pubmed: Author and Title
Google Scholar: Author Only Title Only Author and Title

Sawai, S., and Saito, K. (2011). Triterpenoid biosynthesis and engineering in plants. Front Plant Sci 2, 25.
Pubmed: Author and Title
Google Scholar: Author Only Title Only Author and Title

Sayama, T., Ono, E., Takagi, K., Takada, Y., Horikawa, M., Nakamoto, Y., Hirose, A., Sasama, H., Ohashi, M., Hasegawa, H., Terakawa, T., Kikuchi, A., Kato, S., Tatsuzaki, N., Tsukamoto, C., and Ishimoto, M. (2012). The Sg-1 glycosyltransferase locus regulates structural diversity of triterpenoid saponins of soybean. Plant Cell 24, 2123-2138.
Pubmed: Author and Title
Google Scholar: Author Only Title Only Author and Title

Shao, H., He, X., Achnine, L., Blount, J.W., Dixon, R.A., and Wang, X. (2005). Crystal structures of a multifunctional triterpene/flavonoid glycosyltransferase from Medicago truncatula. Plant Cell 17, 3141-3154.
Pubmed: Author and Title
Google Scholar: Author Only Title Only Author and Title

Shibuya, M., Nishimura, K., Yasuyama, N., and Ebizuka, Y. (2010). Identification and characterization of glycosyltransferases involved in the biosynthesis of soyasaponin I in Glycine max. FEBS Lett. 584, 2258-2264.
Pubmed: Author and Title
Google Scholar: Author Only Title Only Author and Title

Tohge, T., Nishiyama, Y., Hirai, M.Y., Yano, M., Nakajima, J., Awazuhara, M., Inoue, E., Takahashi, H., Goodenowe, D.B., Kitayama, M., Noji, M., Yamazaki, M., and Saito, K. (2005). Functional genomics by integrated analysis of metabolome and transcriptome of Arabidopsis plants over-expressing an MYB transcription factor. Plant J. 42, 218-235.
Pubmed: Author and Title
Google Scholar: Author Only Title Only Author and Title

Tyanova, S., Temu, T., and Cox, J. (2016). The MaxQuant computational platform for mass spectrometry-based shotgun proteomics. Nat Protoc 11, 2301-2319.
Pubmed: Author and Title
Google Scholar: Author Only Title Only Author and Title

Van Der Spoel, D., Lindahl, E., Hess, B., Groenhof, G., Mark, A.E., and Berendsen, H.J. (2005). GROMACS: fast, flexible, and free. J Comput Chem 26, 1701-1718.
Pubmed: Author and Title
Google Scholar: Author Only Title Only Author and Title

Vetter, J. (2000). Plant cyanogenic glycosides. Toxicon 38, 11-36.
Pubmed: Author and Title
Google Scholar: Author Only Title Only Author and Title

Vincken, J.P., Heng, L., de Groot, A., and Gruppen, H. (2007). Saponins, classification and occurrence in the plant kingdom. Phytochemistry 68, 275-297.
Pubmed: Author and Title
Google Scholar: Author Only Title Only Author and Title

Vogt, T., and Jones, P. (2000). Glycosyltransferases in plant natural product synthesis: characterization of a supergene family. Trends Plant Sci. 5, 380-386.
Pubmed: Author and Title
Google Scholar: Author Only Title Only Author and Title

Wang, P., Wei, Y., Fan, Y., Liu, Q., Wei, W., Yang, C., Zhang, L., Zhao, G., Yue, J., Yan, X., and Zhou, Z. (2015). Production of bioactive ginsenosides Rh2 and Rg3 by metabolically engineered yeasts. Metab. Eng. 29, 97-105.
Pubmed: Author and Title
Google Scholar: Author Only Title Only Author and Title

Wei, W., Wang, P., Wei, Y., Liu, Q., Yang, C., Zhao, G., Yue, J., Yan, X., and Zhou, Z. (2015). Characterization of Panax ginseng UDP-glycosyltransferases catalyzing protopanaxatriol and biosyntheses of bioactive ginsenosides F1 and Rh1 in metabolically engineered yeasts. Mol Plant 8, 1412-1424.
Pubmed: Author and Title
Google Scholar: Author Only Title Only Author and Title

Wetterhorn, K.M., Newmister, S.A., Caniza, R.K., Busman, M., McCormick, S.P., Berthiller, F., Adam, G., and Rayment, I. (2016). Crystal Structure of Os79 (Os04g0206600) from Oryza sativa: A UDP-glucosyltransferase Involved in the Detoxification of Deoxynivalenol. Biochemistry 55, 6175-6186.
Pubmed: Author and Title
Google Scholar: Author Only Title Only Author and Title

Xu, G.J., Cai, W., Gao, W., and Liu, C.S. (2016). A novel glucuronosyltransferase has an unprecedented ability to catalyse continuous two-step glucuronosylation of glycyrrhetinic acid to yield glycyrrhizin. New Phytol. 212, 123-135.
Pubmed: Author and Title
Google Scholar: Author Only Title Only Author and Title

Yang, J., Yan, R., Roy, A., Xu, D., Poisson, J., and Zhang, Y. (2015). The I-TASSER Suite: protein structure and function prediction. Nat. Methods 12, 7-8.
Pubmed: Author and Title
Google Scholar: Author Only Title Only Author and Title

Yonekura-Sakakibara, K., Tohge, T., Matsuda, F., Nakabayashi, R., Takayama, H., Niida, R., Watanabe-Takahashi, A., Inoue, E., and Saito, K. (2008). Comprehensive flavonol profiling and transcriptome coexpression analysis leading to decoding gene-metabolite correlations in Arabidopsis. Plant Cell 20, 2160-2176.
Pubmed: Author and Title
Google Scholar: Author Only Title Only Author and Title

Analysis of two new arabinosyltransferases belonging to the carbohydrate-active enzyme (CAZY) glycosyl transferase family 1 provides insights into disease resistance and sugar donor specificity

Thomas Louveau, Anastasia Orme, Hans Pfalzgraf, Michael Stephenson, Rachel E Melton, Gerhard Saalbach, Andrew M Hemmings, Aymeric Leveau, Martin Rejzek, Robert John Vickerstaff, Tim Langdon, Rob Field and Anne E. Osbourn

Plant Cell; originally published online November 14, 2018;
DOI 10.1105/tpc.18.00641